ABSTRACT

LINDA D. MICHAELS. A Study of Particle Bounce in Inertial Impaction Samplers. (Under the direction of Dr. Madhav B. Ranade.)

Environmental and industrial hygiene samples of fine airborne particles are commonly collected in inertial impaction-based devices. In an ideal form these devices aerodynamically separate particles according to their size. It has been known for some time that solid particles with high Stokes numbers are capable of rebounding from impactor substrates and, consequently, distorting the particle size information obtainable from inertial impactors. However, the phenomenon of particle bounce is poorly understood, and little is known about how particle materials and substrates can affect the amount of particle bounce.

In this experiment, a method was developed for the measurement of particle bounce from substrates of three different materials. The particle materials were also varied. The relative bounce of particles over a range of Stokes numbers was compared to literature reported results of similar experiments and to values predicted by a tentative theory of particle capture by surfaces. Experimental results showed good agreement with values expected on the basis of theory. Glass beads showed unexpectedly high collection efficiencies at small Stokes numbers when a dry substrate was used.

AKNOWLEDGMENTS

I would like to take this opportunity to thank all those who have helped in so many ways during this project:

My advisor, Dr. M. B. Ranade, for his ideas, enthusiasm, and wise guidance in this project.

Fred Schwartz and Daryl Smith for construction of the apparatus used in the study.

Andy Viner for his amazing patience and good humor in dealing with the student-computer interface.

My co-workers at the Research Triangle Institute for their ideas, support, encouragement, and many informative discussions--Chloe Smith, Doug VanOsdell, Dr. David Ensor, and Ed Kashdan.

The Research Triangle Institute for their generous support during parts of this work and for the use of their equipment and facilities.

My parents for their constant support and encouragement in all my undertakings, often, even in spite of their better judgements.

TABLE OF CONTENTS

LIST OF TABLES

LIST OF FIGURES

LIST OF FIGURES (continued)

NOMENCLATURE

A	Bradley-Hamaker constant
B_f	Bouncing fraction
C_c	Cunningham slip correction
C_e	Collision efficiency
d	Particle diameter
d_{50}	Particle diameter collected with 50-percent efficiency
D_j	Jet diameter
e	Co-efficient of restitution
E_i	Energy of a particle due to van der Waals attraction
E_r	Energy of a particle on rebounding from a surface
h	Adhesion probability
KE_i	Kinetic energy of a particle incident to a collector
KE_r	Kinetic energy of a particle on rebounding from a surface
K_p	Bulk mechanical property
m	Mass of a particle
N_o	Number of particles colliding with an substrate as a ratio to the number of particles in the challenge air stream
n	Number of replicate samples
OPC	Optical Particle Counter
PSL	Polystyrene latex
$\hat{R}$	Estimate of η based on n number of replicates
Rej	Jet Reynolds number
S	Vertical distance from the exit plane of the jet to the collector surface
Stk	Stokes number
$\sqrt{Stk}_{50}$	The square root of Stokes number corresponding to a collection efficiency of 50 percent

NOMENCLATURE (continued)

U	Average jet velocity at its exit
V_i	Incident velocity normal to a collector
V^*	Critical rebound velocity
V_r	Velocity of a particle on rebound from a surface
W	Diameter of the jet for a round impactor and width of a rectangular jet
ψ	Critical approach parameter
z	Equilibrium distance of a sphere from a plate or cylinder, usually estimated at 4.0×10^{-8} μm
ρ_{air}	Density of air
ρ_o	Density 1 g/cc
ρ_p	Density of particle

A STUDY OF PARTICLE BOUNCE IN INERTIAL IMPACTION-BASED SAMPLERS

by

Linda D. Michaels

1.0 INTRODUCTION

Inertial aerosol impactors are instruments currently in common useage in the fields of industrial hygiene and air pollution monitoring. Airborne particles are drawn through a narrow nozzle, while an obstacle, generally a plate, partially obstructs the air flow at some distance following its exit from the jet. Particles having less inertia are able to follow the air stream as it passes around the obstruction, while those particles with greater inertia, unable to follow the air stream, impact onto the obstacle. Particles small enough to pass the impaction plate can be quantified downstream, by collection on a filter, for subsequent gravimetric analysis, as is most common, or by some other means. Aerodynamic size segregation of particles can be controlled by following well established impactor design criteria (Marple and Willeke, 1976).

For inertial impaction-based devices to be ideal field instruments, the following criteria should be met: (1) the collection efficiency for both solid and liquid particles, having the same aerodynamic equivalent diameter, should be the same; (2) the collection efficiency should be independent of properties of the material being sampled, such as particle hardness; (3) collection efficiency should be reasonably independent of sample loading on the impaction surface; (4) the collection efficiency should be a univalent function of Stokes number as defined in Equation 1.

Early experimenters with impaction devices noted that large solid particles were capable of bouncing off the impaction surface, (Owens, 1922; May, 1945). These large particles become re-entrained in the airstream and are carried over onto the filter or other type of collector. As a result of particle bounce and carry over, impactors do not show equivalent collection efficiencies for liquid and solid particles of the same aerodynamic diameter. Several studies report that impactor substrate loading affects the fraction of particles that rebound from the collector. Incoming particles impact onto accumulated particles and rebound back into the air stream, suggesting that particle bounce is closely related to the hardness and surface structure of the particle material and to that of the surface it impacts on.

A variety of methods have been devised to limit or to prevent particle bounce. Owens (1922) designed a humidifying chamber in his impactor to moisten the dust particles prior to their collision with the impaction plate. More commonly, the impaction surface has been covered with a thin layer of viscous material (May, 1945; Davies et al., 1951; Rao and Whitby, 1978). The addition of a viscous layer has not been entirely satisfactory. The thickness of the layer, the type of fluid used, and the particle loading on the viscous layer play an uncertain role in the reduction of particle bounce from the treated impactor surface at some specific operating conditions (Hamilton et al., 1951; Davies et al., 1951; Fuchs, 1978). When it was recognized that bouncing can occur at sufficiently large velocities even from greased surfaces, Hu (1971) used an ultrafine fibrous filter as an impaction substrate to reduce bouncing. However, the filter substrate adversely alters the shape of the efficiency curve (Willeke and McFeters, 1975). Moving-plate impactors have also been designed primarily to prevent particle bounce from previously deposited material, (May, 1956; Goetz, 1969; Lundgren, 1967).

It has been the common wisdom that particle bounce in impactors occurs primarily at high particle velocities or when the aerosol being sampled contains very large particles. However, Dahneke (1975) reports that particle bounce can occur at impact velocities as low as a few centimeters per second for particles of 5 to 10 μm in diameter, while Hering (1984) observed 95-percent bounce-off for 0.945-μm polystyrene

latex spheres and 70-percent bounce-off for 0.22-μm polystyrene latex spheres.

It is clear from this discussion that the ideal inertial impaction device is not currently available. Efforts to substantially eliminate bounce in convenient field use devices have only been partially successful. In addition, the mechanism of particle bounce is poorly understood, and experimental particle bounce data reported in the literature is based on the use of a variety of different test aerosols and collector surfaces with unknown relative bounce characteristics.

It is the objective of this report to: (1) study the effect of (a) varying particle materials and (b) varying collector materials on the distribution of particle adhesion probabilities in an impactor; (2) compare the results of these experiments to the theory of particle capture proposed by Dahneke (1971); (3) compare the data collected from this study with that reported in the literature for similar experiments; and (4) develop a rudimentary scale of relative bounce for (a) particle materials and (b) collector materials, based on these results and those reported in the literature.

A single stage round jet impactor designed to have a cutpoint of 5 μm was built for the study. Removable collection substrates of pyrex, polished Teflon® and polished stainless steel were used in the impactor. Particle materials tested with these collection substrates were ammonium fluorescein and glass beads.

2.0 LITERATURE SURVEY

2.1 Review of Theory

The mechanism of aerosol size segregation in an impactor can be seen as a two stage process. First, the particle must be transported to the impaction plate. This aerodynamic separation step is considered to be well understood. Marple (1970) has developed a model of fluid flow in an impactor which has been successful in predicting the performance of real impactors. At the second stage, the particle must adhere to the collection surface. This requires the collision to be sufficiently inelastic to dissipate any kinetic energy the particle might have in excess of that energy necessary to attract the particle to the surface. In practice, solid particles impinging on dry hard surfaces do rebound. This phenomenon is relatively poorly understood. Dahneke (1971) has advanced a simple one-dimensional theory to describe the capture of particles by surfaces based on an energy balance analysis. However, no satisfactory confirmation of the theory is currently available. A number of investigators have provided partial experimental support for the theory and are reviewed in Section 2.2 of this report.

Collision efficiency, C_e, as used in this discussion refers to the ratio of particles colliding with the collection surface to the number of particles in the challenge air stream.

$$Ce = \frac{\text{number of particles colliding with collector}}{\text{number of particles in the challenge air}}$$

Adhesion or sticking probability, h, refers to the ratio of particles adhering to the collection surface on collision, to the number of particles in the challenge air stream.

$$h = \frac{\text{number of particles adhering to collector}}{\text{number of particles colliding with collector}}$$

Bouncing fraction, Bf, is equal to 1-h.

η, collection efficiency, is equal to $C_e \times h$, and

$$\eta = \frac{\text{number of particles adhering to the plate}}{\text{number of particles in the challenge air stream}}$$

When all the particles colliding with the plate are collected, h = 1, and the collection efficiency and collision efficiency curves are the same. Calibration of an impactor is designed to determine collision efficiency, relying on the operating assumption that all particles colliding with the collector are captured. Consequently, an impactor calibration curve is often referred to as a collection efficiency curve. This is the case with the theoretical collection efficiency curve in Figure 1-1.

2.1.1 Inertial Impactors

The efficiency of an impactor is defined by its deposition curve (assuming no bouncing), showing the dependence of the fraction of particles collected on their aerodynamic diameter.

Efficiency depends on mean flow velocity in the impactor nozzle, U, and the nozzle width as well as particle aerodynamic diameter. If particle motion is in the Stokes region, then efficiency is a univalent function of the Stokes number.

$$\text{Stk} = \frac{\rho_p \, d^2 \, U \, C_c}{9 \, \mu \, D_j} , \qquad (1)$$

where ρ_p is the particle density, d is the particle diameter, C_c is the Cunningham slip factor, μ is the viscosity of the medium, and D_j is the jet diameter. The $\sqrt{\text{Stk}}$ is proportional to the particle diameter and is generally plotted against collection efficiency. In impactor designs where gas flow is rapidly accelerated through a contracting nozzle, particle velocity may be considerably less than that of the gas and its motion may be occuring outside of the Stokes region. Under these conditions, the efficiency curve for the impactor is no longer a univalent function of Stk. A summary number often used to identify an impactor characteristic is the location corresponding to $\eta = 0.5$, also referred to as the d_{50} or the $\sqrt{\text{Stk}_{50}}$.

The shape of the characteristic, or efficiency curve, is specific to an impactor system and depends, to a degree, on the geometry of the impactor and on the jet Reynolds number, Rej.

$$Rej = \frac{\rho_{air} D_j U_I}{\mu} , \qquad (2)$$

where ρ_{air} is the density of air. The degree of dependence on these factors was investigated by Marple (1970, 1974).

Marple modeled the flow fields in an impactor with the aid of a computer by solving the Navier-Stoke differential equations of motion for several model impactors. This technique allowed the calculation of the vertical and horizontal components of velocity at the point of impact with the collection surface. With velocity expressed as the ratio of particle velocity to average jet velocity, V_i/U, Figure 2-1 shows the horizontal and radial components of velocity for particles entering the impactor at point A, near the jet axis ($0.553 \times D_j$) and E, some distance from the jet axis ($1.464 \times D_j$). Figure 2-2 shows the particle trajectories for particles entering the impactor at the same two points. It can be seen from these two figures that at small Stk values, the vertical velocity component is very small and that the particles traveling with these low velocities are colliding with the plate at very small angles.

This model is of particular relevance to the question of particle bounce in impactors. Several studies have reported the onset of bouncing points from uncoated surfaces at very small impact velocities. From Figure 2-1 it can be seen that V_i, velocity normal to the plate at the point of impact, rises rapidly over the range $V_i/U = 0$ to 0.2. The range of $\sqrt{Stk}$ covered in this rapid velocity increase corresponds to those suggested as appropriate design cutpoints by Marple and Willeke (1974). The design criteria cover a region of Rej in which collection efficiencies are relatively unaffected by small changes in design (from Rej = 500 to 3000). At Rej lower than 500, Marple was able to show that the boundary layer parallel to the plate begins to thicken and the sharpness of the collection efficiency curve deteriorates. This can be seen from Figure 2-3 showing the effect of Rej on the velocity profile

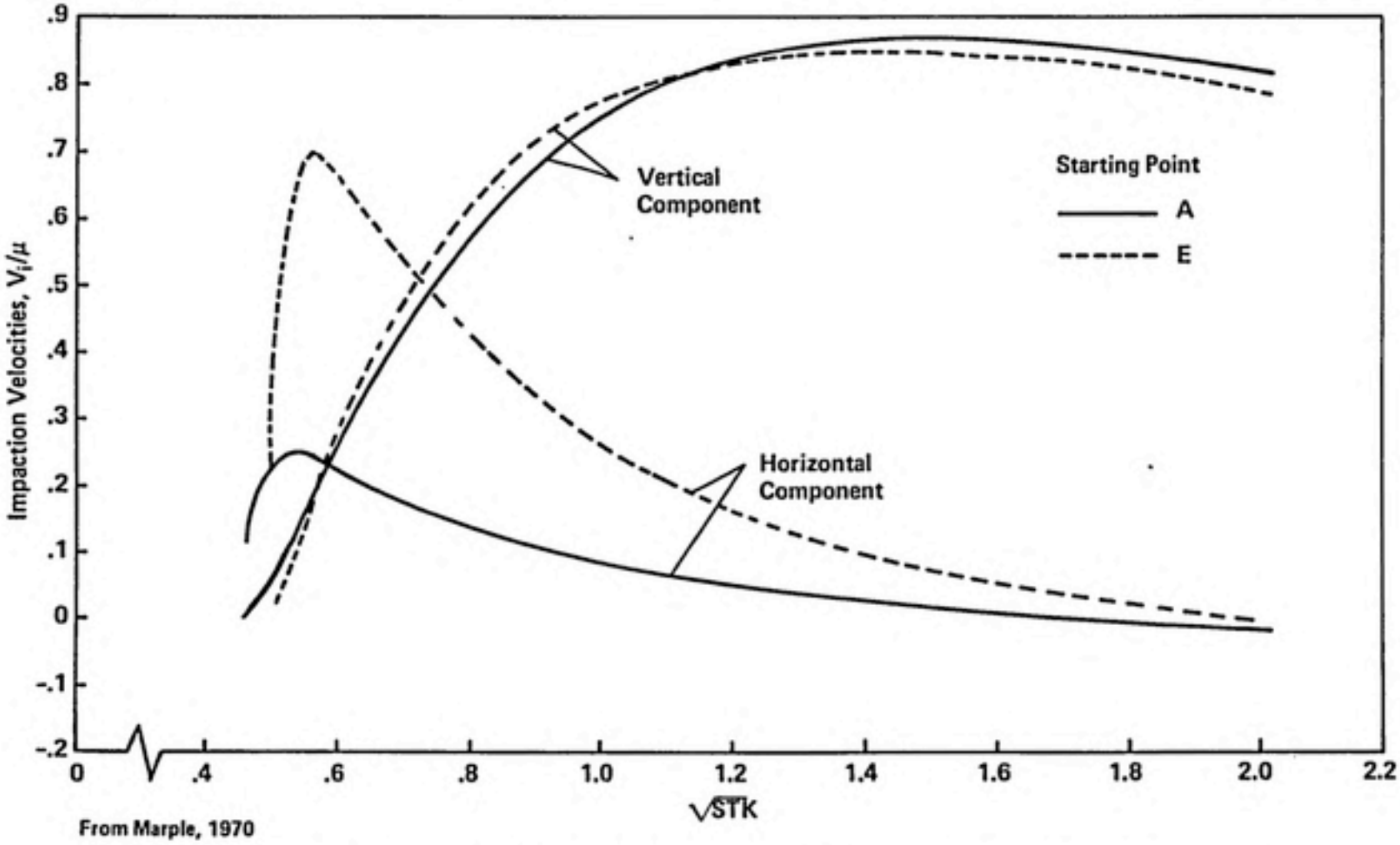

Figure 2-1. Impaction velocities for round impactor at Re = 3000 and S/W = 1/2.

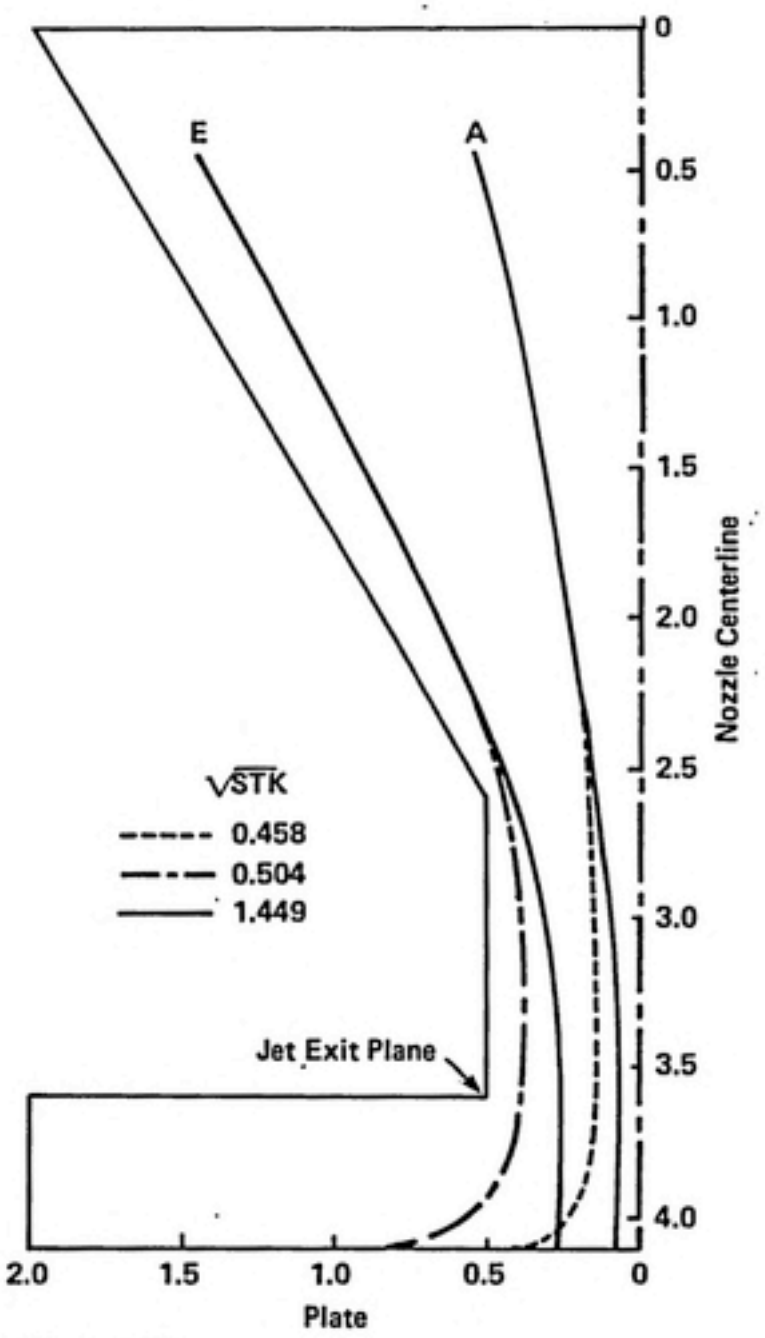

From Marple, 1970

Figure 2-2. Particle trajectories in round impactor.

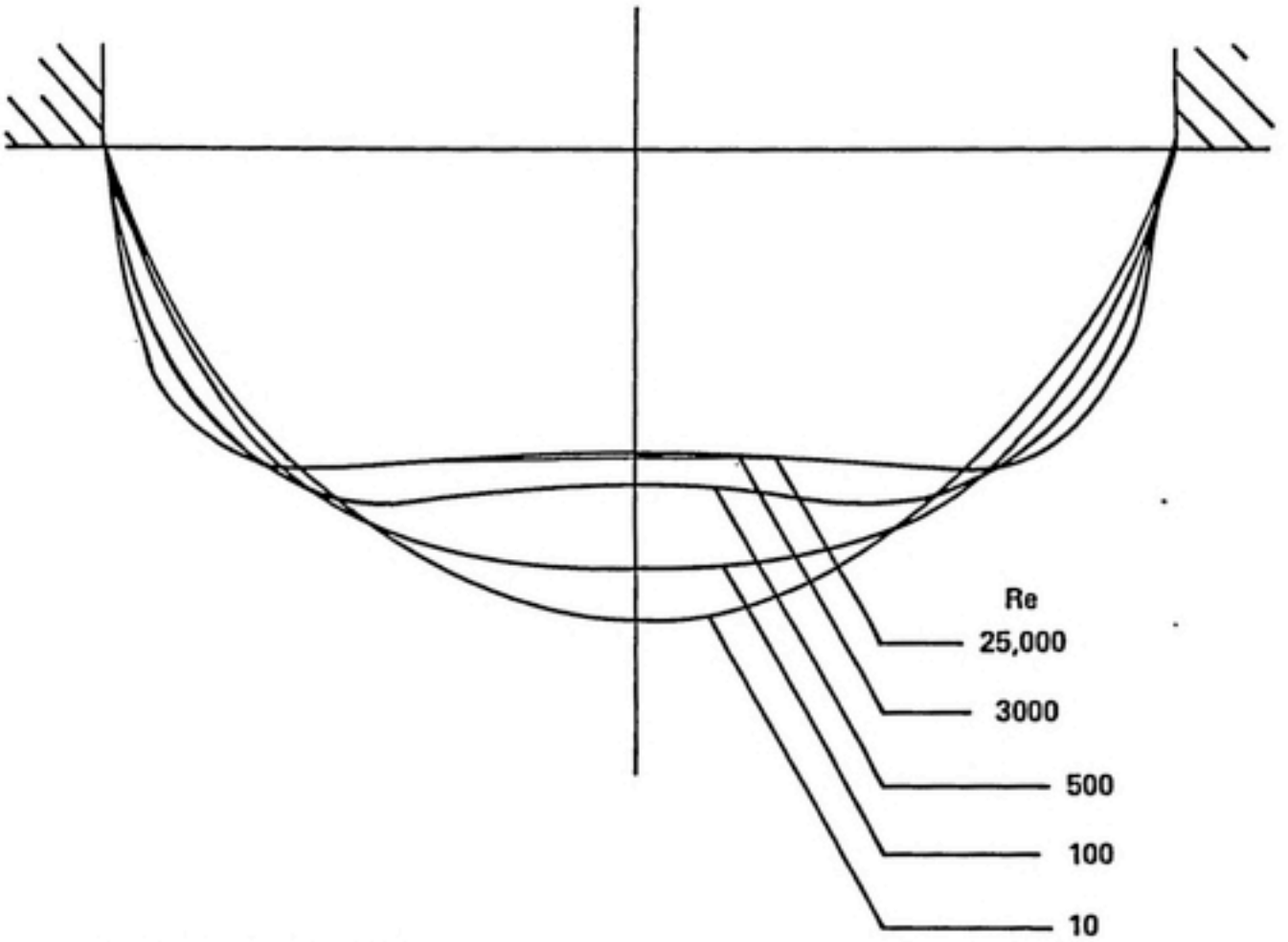

From Marple and Liu, 1978

Figure 2-3. Velocity profiles at the jet exit plane of the round impactor.

at the jet exit and Figure 2-4 showing collection efficiency curves at various Rej's.

For most practical applications, it is desirable to eliminate particle bounce in the range of $\sqrt{Stk}$ up to twice the $\sqrt{Stk_{50}}$, or twice the cutpoint particle diameter. From Figure 2-4, twice an average $\sqrt{Stk_{50}}$ is equal to $\sqrt{Stk}$ of about 0.9.

Using the relation for the critical approach parameter, ψ:

$$\psi = V_i \; d\left(\frac{\rho_p}{\rho_o}\right)^{1/2} = \left[\left(\frac{A}{\pi \; z \; \rho_o}\right)\left(\frac{1 - e^2}{e^2}\right)\right]^{1/2} , \qquad (3)$$

and rearranging it in terms of particles Stokes and Rej:

$$\psi = V_i \; d\left(\frac{\rho_p}{\rho_o}\right)^{1/2} = \left(\frac{3 \; \mu}{\sqrt{\rho_{air} \; \rho_o}}\right)\left(\frac{V_i}{U}\right)\left(\frac{Stk \; Rej}{C_c}\right)^{1/2} , \qquad (4)$$

Hering (1984) substituted an average critical value for ψ, as reported by Cheng and Yeh (1979), of 0.03 cm^2/s and solved for Rej with a $\sqrt{Stk}$ = 0.9, V_i/U = 0.7, and C_c = 1. She found that the Rej must be less than 9 to ensure particle capture at twice the cutpoint.

2.1.2 Particle Capture by Surfaces

Dahneke (1971) developed a simple one-dimensional model of particle collision in which the collision is characterized in terms of the energy of the particle-surface system. A particle approaches a flat surface with a velocity normal to the surface, V_i, with kinetic energy due to V_i, $KE_i = 1/2 \; m \; V_i^2$ where m is the particle mass. The particle is attracted to the surface under the influence of van der Waals potential, E_i, and, consequently, has a total energy of impact at collision of $KE_i + E_i$. A fraction of this energy, e, the coefficient of restitution, is conservatively stored in an elastic collision and is regained on rebound. Kinetic energy at rebound from the surface is therefore equal to $e^2(KE + E_i)$. Part of this energy is used to escape the van der Waals attraction or other attractive forces. When the particle has rebounded beyond the influence of the surface, it has the relative kinetic energy:

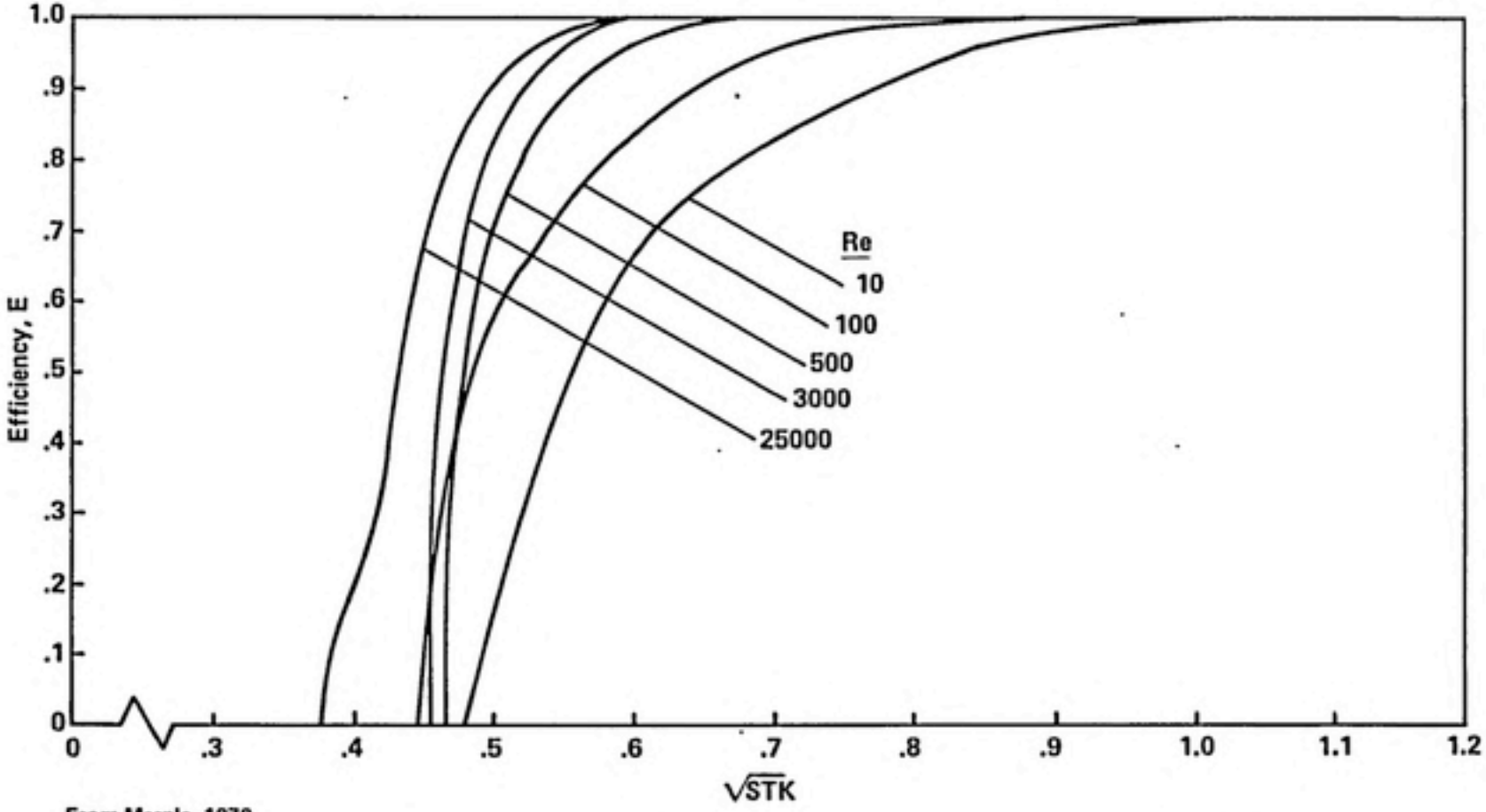

From Marple, 1970

Figure 2-4. Efficiency curves for a round impactor at S/W = 1/2 and five Reynolds numbers.

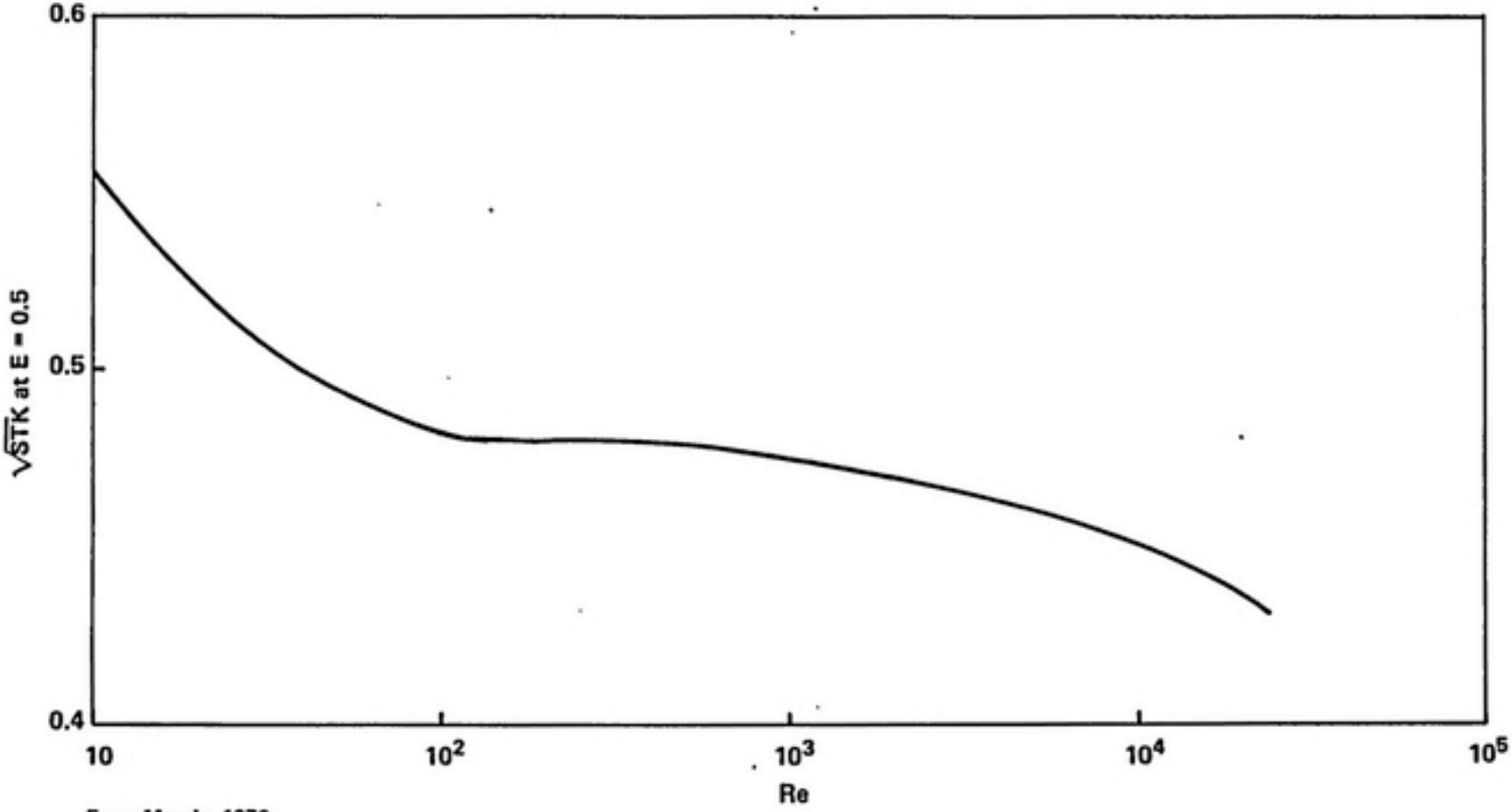

From Marple, 1970

Figure 2-5. Effect of Reynolds number on $\sqrt{STK}$ for a round impactor at S/W = 1/2.

$$KE_r = e^2(KE_i + E_i) - E_r. \quad (5)$$

For simplification, $E = E_i = E_r$. When the particle energy is too low, it will be captured on the surface. With a high V_i, on the other hand, the particle will have sufficient energy to overcome the surface attraction and will bounce. When $KE_r = 0$, particles will be captured. $KE_r > 0$ will lead to particle rebound. A critical velocity, V* which defines this limit between capture and bounce, is:

$$V^* = \left[\frac{2E}{m}\,\frac{(1 - e^2)}{e^2}\right]^{1/2} . \quad (6)$$

E, based on the Bradley-Hamaker theory can be calculated from:

$$E = \frac{Ad}{12z} , \quad (7)$$

where A is the Bradley-Hamaker constant for the sphere-surface combination, d is the particle diameter, and z is the separation between the sphere and the flat. Values for z are generally considered to be 0.0004×10^{-4} cm. Values for A are frequently not known but vary between 10^{-13} and 10^{-12} ergs (Dahneke, 1971).

The dependence of V* on particle diameter can be evaluated from the expression:

$$V^* = \left[\frac{A(1 - e^2)}{\pi\, z\, \rho_p e^2}\right]^{1/2} /d . \quad (8)$$

This relationship is plotted in Figure 2-6.

Several simplifying assumptions are necessary for this evaluation:

1. Viscous drag does not significantly influence particle motion near the surface.
2. The particles are perfectly smooth nonrotating spheres.
3. The surfaces are perfectly smooth, solid, flat, or cylindrical surfaces.
4. The particles approach the surface with normal or near normal incidence.

Coefficients of restitution have been determined experimentally by measuring particle velocity immediately prior to and following the rebound. Then:

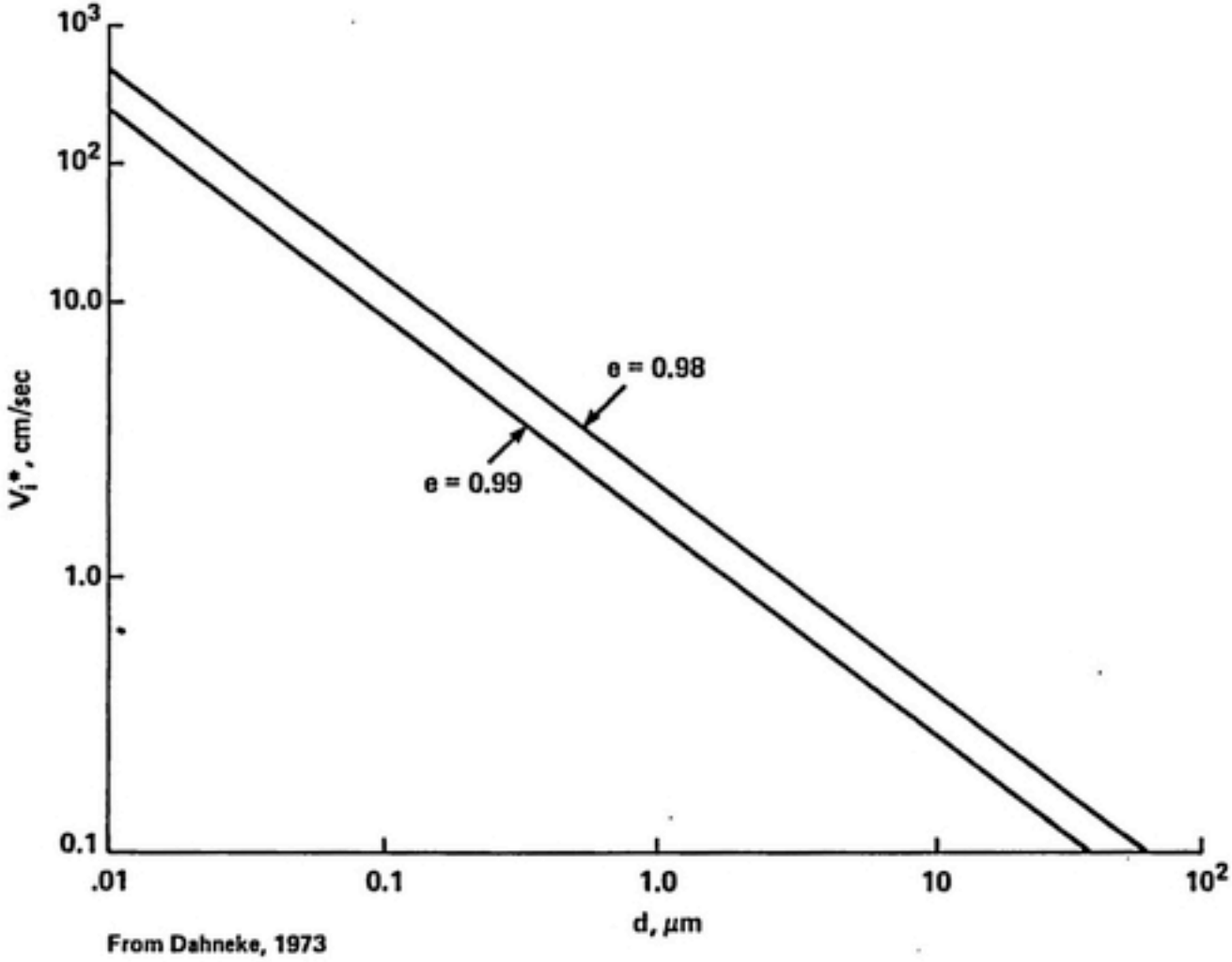

Figure 2-6. The theoretical dependence of critical rebound velocity on particle diameter for silica spheres colliding with a rigid quartz surface.

$$\frac{V_r}{V_i} = \sqrt{e^2 - \left(\frac{2E}{mV_i^2}\right)(1 - e^2)}, \qquad (9)$$

where e is the asymptotic limit of V_r/V_i in the intermediate V_i range, and V_r is the velocity of the particle after impact.

2.2 Review of Experimental Literature

Theoretical work concerning particle bounce has concentrated on prediction of a critical particle velocity above which particles will begin to rebound from an impaction surface. A portion of the experimental work reviewed here attempts to determine a critical velocity and compares the experimentally derived value to that predicted by theory. However, the theory does not provide any distribution of adhesion probabilities. In impactor and filter systems, the critical velocity appears to be so low that bouncing occurs, for all practical purposes, at the same point that collection begins. Consequently, a substantial body of experimental data consists of determinations of adhesion probabilities of particles having velocities greater than the critical velocity. Ultimately, it would be useful to be able to predict adhesion probabilities in a given sampler in order to apply a bounce correction factor to collected data.

Both Dahneke (1973, 1974) and Paw (1983) devised experimental systems to measure adhesion energy of particles traveling at a range of velocities.

Dahneke produced a beam of particles by expanding aerosol through a capillary into a vacuum chamber. The particle beam was directed vertically upward in a vacuum chamber. A deceleration chamber was incorporated into the system where particle beam velocity was controlled by regulating air pressure. Time of flight data for single particles in the beam was collected as a particle passed through a pair of focused HeNe laser beams. In this manner, particle velocity prior to impact with the target and following impact with the target was measured. The coefficent of restitution and the ratio of rebound velocity to incident velocity for that particle/target combination was calculated from the time of flight data. Latex spheres of 0.5 μm to 2.02 μm in diameter and 1.0-μm silica particle beams were directed at

targets of polished quartz, gold on glass, gold foil, and polystyrene. All coefficients of restitution were greater that 0.90, with the exception of very thin gold foil for which the coefficent was 0.45. Coefficients decreased with decreasing particle diameter. The PSL/PSL combination showed the lowest coefficent at 0.90.

The shape of V_r/V_i distributions versus incident velocity for microscopic particles measured over a range of velocities by Dahneke compares favorably with the better understood theory of bounce for large steel balls. The Dahneke theoretical formulation of a simple expression appears to give a good description of small uncharged particle bounce.

Comparison of experimentally determined critical velocities to those expected from theory was disappointing. The theory predicted a value several orders of magnitude smaller than the experimental critical velocities. Possible reasons for the discrepancy, suggested by the author, included the inappropriateness of the Bradley-Hamaker expression to account for the adhesion energy of small PSL spheres, failure to account for elastic flattening, surface effects due to the stabilizer dried on the particles, and contact charging.

Paw generated biological particles into a windtunnel using a simple fluidized bed technique. A cylindrical obstacle with a target material wrapped around it was placed in the tunnel normal to the flow. Particle trajectories were photographed as the particle hit and rebounded from the target surface. From examination of the negatives and comparison with objects of known size, data consisting of distances that particles bounced from the target, the number of particles impinging on the target in a given region of the photograph, and the number of particles bouncing from the target in the same region of the photograph--all as a function of wind speed--was collected. A Runge-Kutta computer program was formulated to convert the raw data to particle velocity normal to the target before and after impingement. From these velocities the coefficients of restitution were determined. Resultant values are listed in Table 2-1.

Plots of V_r/V_i versus impingement velocity for the biological particles showed considerably more scatter than did those developed by Dahneke for PSL spheres, as might be expected for the less uniform

TABLE 2-1. SUMMARY REVIEW OF PERTINENT LITERATURE REPORTED EXPERIMENTS

Reference	Dp	Impactor Type	Re	Experimental Surface	Velocity	Particle Material	Results
Dahneke (1973)	1.27 μm	target surface in a vacuum	--	304 Stainless Steel-polished Quartz polished	--	PSL	Velocity above which bouncing predominates: -83 cm/s for stainless steel; -91 cm/s for polished quartz e = 0.960 on quartz; using: $V^* = \left(\frac{2E}{m}\frac{1-e^2}{e^2}\right)^{1/2}$ gives a theoretical V^* = 6.3 cm/s, ~ 2 orders of magnitude smaller than experimental value. Develops experimental procedure for measuring adhesion energy rather than adhesion force.

(continue)

TABLE 2-1 (continue)

Reference	Dp	Impactor Type	Re	Experimental Surface	Velocity	Particle Material	Results
Loeffler (1974)	3 μm 5 μm 10 μm 5.85 μm 2.75 μm 2.15 μm 1.80 μm 1.25 μm	single fiber	.63-2.51	Polyamide fiber Glass fiber	---	glass quartz paraffin	Lowest adhesion to harder glass fiber Highest adhesion: paraffin, quartz, glass Quartz are irregularly shaped and it appears shape enhances adhesion more than hardness enhances rebound. Small paraffin particles appear to exhibit partly elastic behavior Onset of bounce: 10 μm - 0.03 m/s glass spheres on polyamide fiber 5 μm - 0.05 m/s Theoretical and experimental critical velocities compare favorably. Electrostatic forces appear to make a large contribution to the transport process as the particles approach the fiber.

(continue)

TABLE 2-1 (continue)

Reference	Dp	Impactor Type	Re	Experimental Surface	Velocity	Particle Material	Results
Dahneke (1975)	0.50 μm PSL 0.81 μm PSL 1.27 μm PSL 1.27-.81 μm PSL 2.02 μm PVT .51 μm silica	target in vacuum	--	polished quartz gold/glass polystyrene gold foil polished quartz	Various to 300 m/s	polystrene latex polyvinyltoluene silica	Measured experimental coefficient of restitutions for various sized particle materials on various surfaces. The general shape of the curve of Vreflected/Vincident showed good agreement with energy balance based on theory of larger steel ball bounce. Magnitude off by several orders of magnitude. Suggest adhesion energy of PSL is much greater than predicted by classical theory. Vcritical for 1.27 μm PSL on quartz ~ 120 cm/s. Vcritical for 1 μm silica on quartz ~ 10 cm/s. Larger particles lost less energy in the bounce than smaller particles.

(continue)

TABLE 2-1 (continue)

Reference	Dp	Impactor Type	Re	Experimental Surface	Velocity	Particle Material	Results
Rao & Whitby (1978)	1.1 μm 1.01 μm .794 μm .79 μm .822 μm	round jet single stage impactors	--	glass oil and adhesive coated glass glass fiber filters Whatman filters	--	polystyrene latex	Bounce significant from all but oil-coated surfaces. Dry surfaces showed a maximum collection efficiency from 20-50% and then dropped off with increasing particle diameter. Glass fiber filter reduced bounce (over dry glass plate), but alters collection efficiency characteristic. Loading study: on oiled plate, as collected layer increased, collection efficiency increased; suggests a wicking of oil accounts for increased efficiency. Concludes: 1) stage material significantly influences collection efficiency; 2) theoretical stage cutpoints are not applicable in general. Calibration is necessary.

(continue)

TABLE 2-1 (continue)

Reference	Dp	Impactor Type	Re	Experimental Surface	Velocity	Particle Material	Results
Esmen et al. (1978)	4.4 μm 6.2 8.8 11.6 12.4 15.4	single jet single (removable) stage impactor	--	brass - ASTM B36 aluminum - ASTM B221 coated with carbon black	--	solid uranine	Calculates bouncing fraction by counting footprints left on carbon black by bounced particles and particles retained on the impaction surface. Impact energies calculated using Marple's solution for impact velocities. Good correlation between bouncing fraction vs. impact energy. Maximum adhesion energies aluminum: $0.477\text{-}10.0\times10^{-8}$ ergs brass: $0.350\text{-}5.6\times10^{-8}$ erg From experimental data: $A_{Al} = 9.76\times10^{-13}$ ergs $A_{Brass} = 8.91\times10^{-13}$ ergs $Z = 4.26\times10^{-8}$ cm; showing good agreement with independently established values. Brass bouncier than aluminum.

(continue)

TABLE 2-1 (continue)

Reference	Dp	Impactor Type	Re	Experimental Surface	Velocity	Particle Material	Results
Cheng and Yeh (1979)	11.9 μm 5.70 μm 3.40 μm 2.02 μm 1.01 μm 0.822	radial slit jet (Sierra) - cascade	667-774	uncoated stainless	--	polystyrene latex	Uses various size PSL spheres at a range of $\sqrt{Stk}$. Semi-empirical method to determine V*:

dp (μm)	$\sqrt{Stk}$	V* (cm/s)	Vi/U
5.7	0.455	43.3	0.111
3.40	0.467	88.1	0.137
2.02	0.486	184	0.177
1.011	0.486	355	0.177
0.822	0.501	551	0.209

Bounce from uncoated stainless steel plate begins at or slightly above each stage's cut-point.
Collection efficiency peaks at from 35-55% and reaches a minimum at $\sqrt{Stk} \approx 0.6$ going as low as 5%.
Wall loss studies show bouncing increases wall losses by ≈ 50% at $\sqrt{Stk} \approx 0.8$ and ≈ 14% at smaller particle sizes.

(continue)

TABLE 2-1 (continue)

Reference	Dp	Impactor Type	Re	Experimental Surface	Velocity	Particle Material	Results
Ellenbecker et al. (1980)	Flyash: cmd 0.14 μm σ_g = 1.9 DOP: cmd 0.7 μm σ_g = 2.05	stainless steel fiber filter - 310 stainless steel	--	stainless steel fiber	1.0-8.0 m/s	flyash DOP	Collection efficiency the same for liquid and solid particles until ≈ $\sqrt{Stk}$ of 1, where maximum efficiency is reached. Theoretical efficiency and liquid particle efficiency are in agreement. Increase in velocity shows further decrease in collection efficiency which is most marked at high Stk Plot of particle kinetic energy against adhesion probability shows good correlation with high probability below ≈ 10^{-15} J and low probability above ≈ 10^{-13} J. Scatter of points increased with increasing kinetic energy.

(continue)

TABLE 2-1 (continue)

Reference	Dp	Impactor Type	Re	Experimental Surface	Velocity	Particle Material	Results
Paw (1983)	20-40 μm	covered wooden cylinder in low speed wind tunnel	--	leaf sections: -American elm -tulip poplar glass	Various to ~ 5 m/s	lycopodium spores ragweed pollen glass beads	Experiment at 60% RH to eliminate charging effects. Particles introduced isokinetically to wind tunnel wind speed. Particle size distribution for glass beads not specified. Found that all the particle types rebounded from surfaces at a characteristic critical impact speed regardless of surface type. Coefficient of restitution determined: Glass Lycopodium Ragweed 0.825 0.636 0.514 average from all surfaces. Adhesion energy: Glass: 7.29×10^{-5} erg; Lycopodium: 2.78×10^{-5} erg Ragweed: 6.78×10^{-5} erg Critical velocity: Glass: 0.28 m/s Lycopodium: 0.61 m/s Ragweed: 2.87 m/s. Concludes: 1) critical rebound speeds appear to depend on particle type and be relatively independent of surface type; 2) Bradley-Hamaker adhesion theory estimates adhesion energies at higher than experimentally derived data by several orders of magnitude.

(continue)

TABLE 2-1 (continue)

Reference	Dp	Impactor Type	Re	Experimental Surface	Velocity	Particle Material	Results
Hering (1984)	1.8 μm	Battelle - single round jet per stage Cascade	560-2200	oiled glass frit dry glass oiled filter dry filter	--	potassium bromide PSL	Oiled glass frit (Ace Type E) shows no bounce and no loading effects. Dry glass collection efficiency peaks ≈ 60% at a $\sqrt{Stk}$ ≈ 4.5. Dry filter shows a peak 38% at a $\sqrt{Stk}$ at 0.4. No interference with chemical analysis with oleic acid-coated glass frit.

surface structures of the spores and pollens. However, the general shape of the curves resembled the Dahneke curves, supporting the selection of Runge-Kutta modeling technique.

Coefficients of restitution calculated for the biological particle/target combination were low, which is consistent with the intuitive sense of rebound from a thin, soft leaf target. Dahneke also found that thin gold foil showed very much reduced coefficient of restitution compared to the gold on a rigid glass substrate target. Pollen particles on a glass target had a low coefficient of restitution. The ragweed pollen particles appear to be less prone to bounce (compared to a similar but smooth particle) despite spiney surface protrusions which might be expected to contribute to particle bounce by reducing the area on the particle surface in contact with the target's surface.

Critical rebound velocities for all particle materials tested by Paw were lower than the those reported by Dahneke. Paw used particles of 20 to 40 μm diameter. Since critical velocity is proportional to the inverse of particle mass (Equation 6) larger particles would be expected to have much lower critical rebound velocities than micron-sized particles.

Paw reported no significant difference in critical rebound velocity for different target surfaces while very significant differences were present in critical rebound velocities among the three particle materials studied. This observation has not been supported by the work of other investigators (Hiller and Loeffler, 1974; Rao and Whitby, 1978; Esmen et al., 1978; Hering, 1984).

Paw does not provide sufficient information to establish whether heavy target loading conditions were present during the windtunnel testing. However, when heavy loading of the target occurs, the target surface becomes a layer of the particles. The particle-target material interaction is replaced by a particle-particle layer interaction. Such conditions may account for the apparent lack of difference between glass and leaf targets. A variety of altered collection efficiency effects have been attributed to the loading of particles on the target surface. Rao and Whitby (1978) found that collection efficiency was increased when a heavy deposit of PSL bead was formed on an impactor

surface (possibly due to wicking of the oil used to enhance adhesion of the loading layers of particles), while Reischl and John (1978) and Hering (1984) found that particle loading decreased collection of a substrate using PSL or potassium iodide particles. In the pilot study report in Appendix A, collection efficiency of ragweed pollen particles and 20-μm ammonium fluorescein particles on greased stainless steel under heavy loading conditions were compared. When ammonium fluorescein particles essentially impacted on ammonium fluorescein particles, collection efficiency dropped rapidly approaching the level of bounce found on bare stainless steel plates. Ragweed pollen collection efficiency remained constant under heavy loading conditions and was comparable to the collection efficiency obtained under normal loading conditions with a greased collection substrate. Evidently, the pollen particles collected themselves effectively, while the ammonium fluorescein particles provided a very bouncy target surface for themselves. Similar particle-particle collection characteristic differences may account for differing observations concerning particle loading effects.

Paw's calculations of adhesion energies, using Bradley-Hamaker theory, were reported to be high by comparison to the experimentally measured adhesion force for the same particle surface-pairs by a factor of 4 to 200 times, even after adjustment was made to account for the larger z (as measured by scanning electron microscopy) of 1 μm.

Esmen et al. (1978) selected an impactor system to examine the relationship between theoretically and experimentally derived adhesion energies. While the use of impactors to this end are limited due to the complexities involved in the calculations of impact energies, Esmen was able to show excellent experimental agreement with Dahneke's theory.

Fraction of particles bouncing from an aluminum and a brass substrate were determined by optical microscope counting of "footprints" left on a thin layer of carbon black on the impaction surface by particles which struck but failed to adhere to the plate. Impaction energy of particles striking the surface was calculated using Marple's method, and from these, impact energy was calculated. The square root of the fraction of particles bouncing correlates extremely well with

the calculated impaction energy in the case of both substrate materials, with the harder brass showing lower impaction energy required for a given bouncing fraction as would be expected.

By extrapolating the bouncing fraction back to 0, the maximum energy of adhesion was determined for each particle size and substrate. These values vary from $.477 \times 10^{-8}$ to 10×10^{-8} ergs for aluminum and 0.350×10^{-8} to 5.60×10^{-8} ergs for brass. In order to verify experimental and theoretical agreement, values for particle bulk mechanical property, Kp, Bradley-Hamaker constants, A, and separation distances between particle and surface, z, were calculated from the experimental data and compared with independantly reported values. In addition, if Dahneke's theory is consistent, values of A/z and ratios of diameter and energy to their dimensionless counterparts should be constant over the experimental conditions. Reasonably good agreement was found in all these tests of experimental agreement with theory. The experimentally determined values of for A were 9.76×10^{-13} ergs for aluminum, 8.91×10^{-13} ergs for brass, and for z, 4.26×10^{-8} cm.

Ellenbecker et al. (1980) and Loeffler (1974) examined particle bounce from fibers. Ellenbecker measured bounce of fly ash particles from mats of stainless steel fibers in the 1- to 8-m/s particle velocity range. When particle kinetic energy was plotted against adhesion probabilities, a reasonably good correlation was seen with scatter increasing as particle kinetic energy increased. Considering difference in particle shape and impaction surface geometry, good agreement was observed when compared to Esmen's data for bounce from a brass plate.

Loeffler measured adhesion probabilities of glass, quartz, and paraffin particles on polyamide and glass single fibers. From theory, a plot of critical particle velocity versus particle diameter at coefficients of restitution ranging from 0.1 to 1.0 was produced. High speed photographs of particle trajectories in the vacinity of the fiber enabled the calculation of the coefficients of restitution and experimental critical rebound velocities. Critical velocities for quartz particles were 15 and 8 cm/s, and for glass spheres were 5 and 3 cm/s for 5- and 10-μm particles, respectively. These velocity compared favorably with those predicted by theory.

Cheng and Yeh (1979) used a semi-empirical method to predict the onset of particle bounce in a Sierra radial slit jet impactor. The collection efficiency of each impactor stage was measured with adhesive coated stainless steel plates and PSL spheres. The procedure was then repeated with uncoated steel plates over a range of particle $\sqrt{Stk}$ from 0.3 to 0.8. Impact velocities at the stagnation point of the collection surface were modeled over the range of $\sqrt{Stk}$ using approximations proposed by Mercer and Chow (1968) and Mercer and Stafford (1969). Critical rebound velocities were calculated using Dahneke's theoretical formulations. On the first stage, rebound occured at $\sqrt{Stk}$ of 0.455, which corresponded to a velocity of 43.3 cm/s. The highest critical rebound velocity was 551 cm/s in the last stage. Cheng and Yeh found that no critical rebound velocity, expressed in units of average jet velocity, exceeded 0.209.

A general formulation of minimum impact velocity:

$$V_i \, d < 5 \times 10^{-6} \ m^2/s,$$

was advanced to limit the occurrence of bouncing to particles that are larger than the stage cutpoint size.

In addition to determining a critical rebound velocity, the work of Cheng and Yeh provides some insight into the adhesion probability distribution for the impactor system. Adhesive coated stages were not successful in completely eliminating bouncing. The collection efficiency on all coated stages never exceeded 89 percent, while liquid DOP particle efficiencies reached near 100 percent on all impactor stages. On all but the stage labeled No. 4, bouncing began at or slightly above the stage cutpoint. In stage No. 4, with a cutpoint of 1.0 μm, collection efficiency was reduced to approximately 35 percent at the theoretical 50-percent collection efficiency point. All of the collection efficiency curves for bare stainless steel plates had a similar shape with a maximum collection efficiency occuring at a slightly larger $\sqrt{Stk}$ than the cutpoint, with values ranging from approximately 35 to 55 percent and dropping off rapidly to minimums of from 5 to 25 percent at a $\sqrt{Stk}$ of about 0.6.

The Cheng and Yeh data describing bouncing distributions accurately reflects the work of other investigators (Rao and Whitby, 1978;

Esmen, 1978; Ellenbecker et al., 1980; Hering, 1984). Collection efficiency curves collected in all the work reviewed follow the the "no bounce" curve up to some point near the impactor cut point and then drop sharply to a minimum. Hering (1984) reported the collection efficiency of 1.8-μm potassium bromide particles on both dry glass and Teflon® filter impaction surfaces dropped to a minimum of near 0 percent at a $\sqrt{Stk}$ of less than 0.8. Ellenbecker et al. (1980), calculating the single fiber collection efficiency from tests using a stainless steel filters (not in an impactor), found the same minimum to occur for fly ash particles sampled at a velocity of 8.0 m/s at close to a $\sqrt{Stk}$ of 100. However, for fly ash particles sampled at a velocity of 1.5 m/s, even at $\sqrt{Stk}$ greater than 100, the minimum collection efficiency did not drop below 20 percent. Rao and Whitby (1978) found the minimum to occur at $\sqrt{Stk}$ close to 0.55 with an efficiency of about 25 percent for 1.10- and 1.011-μm PSL particles on uncoated glass. The collection efficiency rose after this minimum was reached up to approximately 30 percent at a $\sqrt{Stk}$ of 0.65 where data collection ended.

Several investigators have examined the effect of impactor surfaces on particle bounce. Rao and Whitby (1978) compared bounce characteristics of PSL particles on oil coated glass, glass fiber filters, Whatman filters, and bare glass. The untreated glass showed extensive bounce, never exceeding a collection efficiency of 55 percent, while the oil coated glass appeared to have collection characteristics approaching those of Marple's theoretical impactor. The glass fiber filter reduced bounce somewhat; however, collection efficiency did not exceed 75 percent. The Whatman filter showed generally poor collection characteristics. Both the glass fiber and bare glass impaction surfaces were more efficient than predicted on the basis of impaction alone at $\sqrt{Stk}$ below about 0.45. This latter point tends to suggest other collection mechanisms are at work in the region below the impactor cutpoint. Loeffler (1974) made a similar observation with glass particles collected on glass filters and concluded that electrostatic forces made a large contribution to the transport process as the particles approach the filter. In a subsequent study, Loeffler (1975) modeled single fiber collection efficiency taking into account electrostatic, inertial, and gravitational forces in a Lamb's flow

field. The resulting theoretical collection efficiency curves show increased efficiencies would be expected (as compared with the model neglecting electrostatic force) at low $\sqrt{Stk}$, dipping to a minimum at some point less than $\sqrt{Stk} = 1$. The model, including electrostatic forces, then parallels the model which excludes the latter effect. Investigation with charged particles, charged fibers, and real filters supported the conclusion that electrostatic effects can modify collision efficiency .

Esmen et al.(1978) found that a brass impaction surface in an impactor resulted in a larger fraction of particles bouncing than did an aluminium plate under comparable conditions. Dahneke (1974) reported a higher critical rebound velocity for quartz than for stainless steel impaction targets. The rigidity of the impaction surface was also noted as a factor affecting relative bounce. Dahneke noted that the coefficient of restitution for thin gold foil was approximately half the value for a thin gold layer on a rigid glass surface. These observation are consistent with information on the relative hardness of materials (Mohs hardness scale values are listed in Table 2-2).

TABLE 2-2. Mohs Scale of Hardness for Selected Materials

Material	Mohs Hardness Scale
Quartz	7
Steel	5 - 8.5
Glass	4.5 - 6.5
Brass	3 - 4
Gold	2.5 - 3
Aluminium	2 - 2.9
Wax (0 C)	0.2

Source: CRC Handbook of Physics and Chemistry, 52nd Edition.

Corn and Stein (1965) found that particle adhesion was reduced on rough surfaces. Further, relative humidity greatly affected adhesion of glass beads and fly ash to a glass surface. He found that a force

of 0.66 dyne was required to remove 50 percent of adhering 37-μm particles at a relative humidity of 35 percent, while at a relative humidity of 75 percent, 0.96 dynes were required to remove the same proportion of 37-μm particles.

Very little information has been collected on the relative bounciness of particle materials. Loeffler (1974) observed that quartz particles showed less bouncing than did smooth glass spheres even though quartz is a harder material. This was attributed to a particle shape effect. Irregular quartz particles would have a larger number of contact points than the smooth glass spheres. Paraffin wax particles were found to be somewhat bouncier than might be expected, falling in the same range of adhesion probabilities as did the quartz particles. The wax spheres appear to exhibit a partly elastic behavior at the microscopic size level. Loeffler verified this latter observation by repeating impaction tests with a tacky fiber. Paraffin particle adhesion was greatly increased under these conditions. In the pilot study reported in Appendix A, the collection efficiency of a stainless steel impaction plate with 20-μm particles of ammonium fluorescein, glass beads, and ragweed pollen was compared. The particles were collected with efficiencies of 38 percent, 52 percent and 78 percent, respectively. The same relative bounciness of ragweed pollen and glass beads collected on a glass target was noted by Paw (1983).

Summary

A review of experimental literature shows general agreement on the nature of solid particle bounce from impaction surfaces whether they be fibers or plates. A variety of target and particle characteristics have been reported to affect the fraction of particles bouncing in a given system. In general, the properties of the surface that have been shown to affect collection efficiency are surface hardness, particle loading on the surface, other surface coating such as water, greases, surface roughness, and rigidity of the surface. Particle material characteristics were observed to affect the collection efficiency of a given system. Particle hardness may play some role in this; however, determining hardness on the scale of a microscopic particle has not

been attempted in the studies reviewed. Irregular particle shape was reported to reduce particle bounce.

Other particle material characteristics have also been reported to affect the fraction of particles bouncing in all but one of the studies reviewed.

Determination of critical rebound velocities was attempted in fundamental studies, as well as semi-empirically in impactor systems and with single fibers. Because of the range of experimental conditions involved, it is difficult to comment on overall agreement. Table 2-3 summarizes experimental and theoretical values from the literature for critical rebound velocity and experimental values for coefficients of restitution. Most researchers claimed good agreement with theory. In all cases reasonable correlations between particle kinetic energy at impact and adhesion probability were reported.

TABLE 2-3. COMPARISON OF LITERATURE REPORTED VALUES FOR COEFFICIENT OF RESTITUTION AND CRITICAL REBOUND VELOCITY

Reference	Particle Material	Diameter (μm)	Collector Material	e	V* (cm/s) Experimental	V* (cm/s) Theoretical
Dahneke (1971, 1973, 1975)	PSL	1.27	polished quartz	0.960	120, 91	- , 6.3
	Silica	1.0	polished quartz	--	< 10	
	PSL	0.81	polished quartz	0.90		
	PSL	0.50	polished quartz	0.93		
	Silica	0.51	polished quartz	≈ 0.92		
	PSL	1.27	gold on glass	0.930		
		0.81	gold on glass	0.90		
	PSL	0.81	PSL	0.90		
	PSL	1.27	polished stainless steel	< 0.960	83	
Paw (1983)	Glass	20-40	glass	0.950	25	
	Glass	20-40	leaf	0.763-0.828	26-31	
	Lycopodium Spores	20-40	glass	0.816	62	
			leaf	0.556-0.634	51-69	
	Ragweed Pollen	20-40	leaf	0.395-0.577	221-347	
Loeffler (1978)	Quartz	5	polyamide	≈ 0.95	15	4-10
	Glass	5	polyamide	≈ 0.95	5, 6	
	Wax	10	polyamide	--	10	
	Quartz	10	polyamide	0.82	8	2-5
	Glass	10	polyamide	0.82	3	2-5
Broom (1979)	Glass	4.7	steel	--	9.8	
Cheng & Yeh (1979)	PSL	5.7	stainless steel	≈ 0.95	43.3	
	PSL	3.40			88.1	
	PSL	2.02			184	
	PSL	1.011			355	
		0.822			551	

3.0 EXPERIMENTAL METHODS

3.1 Pilot Study

A pilot study was undertaken to select appropriate methods and experimental designs for the examination of particle bounce in inertial impaction devices. A stainless steel and brass impactor (with a removable stainless steel collector) was friction fitted to the inlet probe of a Climet Model 208 light scattering Optical Particle Counter (OPC). The OPC was modified to permit detection of particles larger than 20 μm in diameter and to permit an interface with a Radio Shack TRS-80 computer which was used to acquire and manipulate data. Particle materials used in the study were glass beads, ragweed pollen, and ammonium fluorescein. Details of the pilot study experiment are contained in Appendix A.

Based on the findings of the pilot study, the following factors were considered in the design of the final experiments: (1) The OPC was a reasonable method of analyzing particle bounce information using the above particle materials. Differences in the penetration of the three materials were detectable with the OPC and were found to be signicantly different from each other. (2) Particle loading on the collector affects particle penetration through the impactor replacing measurements of particle-collector effects with particle-particle effects. To minimize uncertainty concerning the presence of loading effects, the challenge concentration should be maintained at the minimum necessary for reasonable detection. (3) The fluidized bed used to generate glass beads in the pilot study was unable to provide a constant aerosol concentration for any period in excess of 10 minutes. This was due to the reduction in the load of beads available for suspension in the bed over time. It was noted that the same generation system delivered a constant concentration of ragweed pollen over a period of time in excess of 25 minutes. Some other technique, capable

of producing a constant concentration of glass beads over a period of time in excess of one hour, would be necessary.

3.2 Methods

The collection efficiency of a given particle-material combination was determined in the current study with a Climet OPC. Monodisperse ammonium fluorescein particles were generated using a TSI Model 3450 vibrating orifice aerosol generator. Glass beads were generated with a modified Timbrell asbestor generator (Timbrell et al., 1968). The aerosol was passed through a 10-mCi Kr-85 source charge neutralizer (TSI Model 3054) before being sampled by the impactor. The optical OPC was located immediately downstream of the impactor. To reduce the concentration of particles in the sample, the aerosol was diluted with clean dry filtered air introduced through a porous tube diluter upstream of the impactor. The experimental set-ups are diagrammed in Figures 3-1 and 3-2.

The use of an OPC to evaluate particle penetration offers the advantages of near real-time data collection and short duration sampling periods. The short sample duration allows the acquisition of a large data base requiring no further laboratory analysis. In combination with the addition of dilution air, short sampling periods prevent the buildup of sampled material on the substrate.

The "no bounce" case was determined by generating liquid oleic acid-uranine particles and counting the number of particles passing the various substrates. Since the oleic acid particles were generated as monodisperse aerosol, a second "no bounce case" was established for the polydisperse glass beads by adding an oleic acid soaked glass frit (Ace Glass, type E filter disc) collector to the randomized test series. Hering (1984) reported excellent particle capture characteristics for a similar oiled glass frit, and she found no apparent particle buildup effect with the substrate. The calibration curve generated with the glass frit and glass beads was compared to the oleic acid-uranine calibration curve. In addition, the glass frit was added to the 7-μm ammonium fluorescein sampling series to allow comparison of collection efficiency on the glass frit between particle materials.

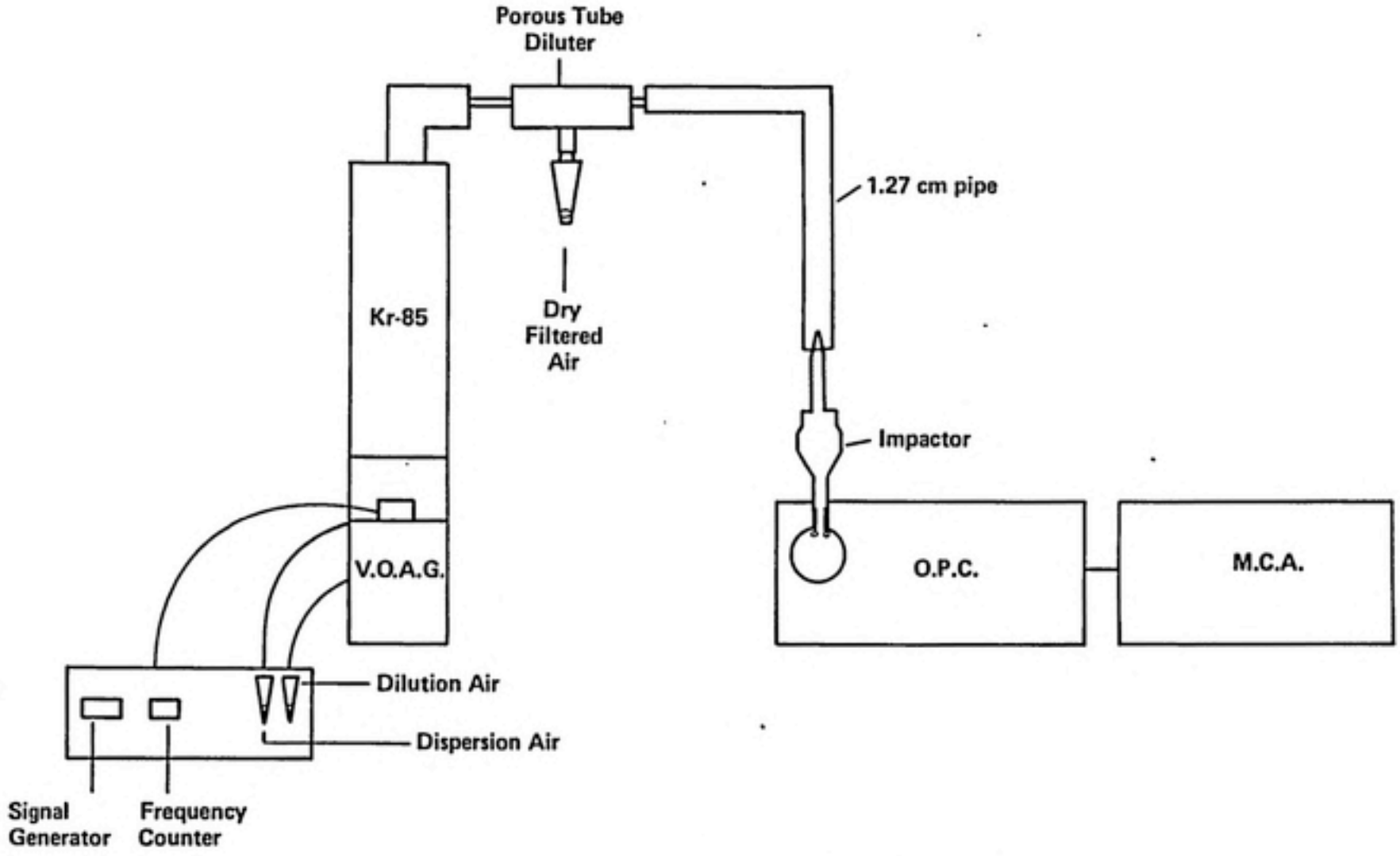

Figure 3-1. Experimental configuration using vibrating orifice aerosol generator.

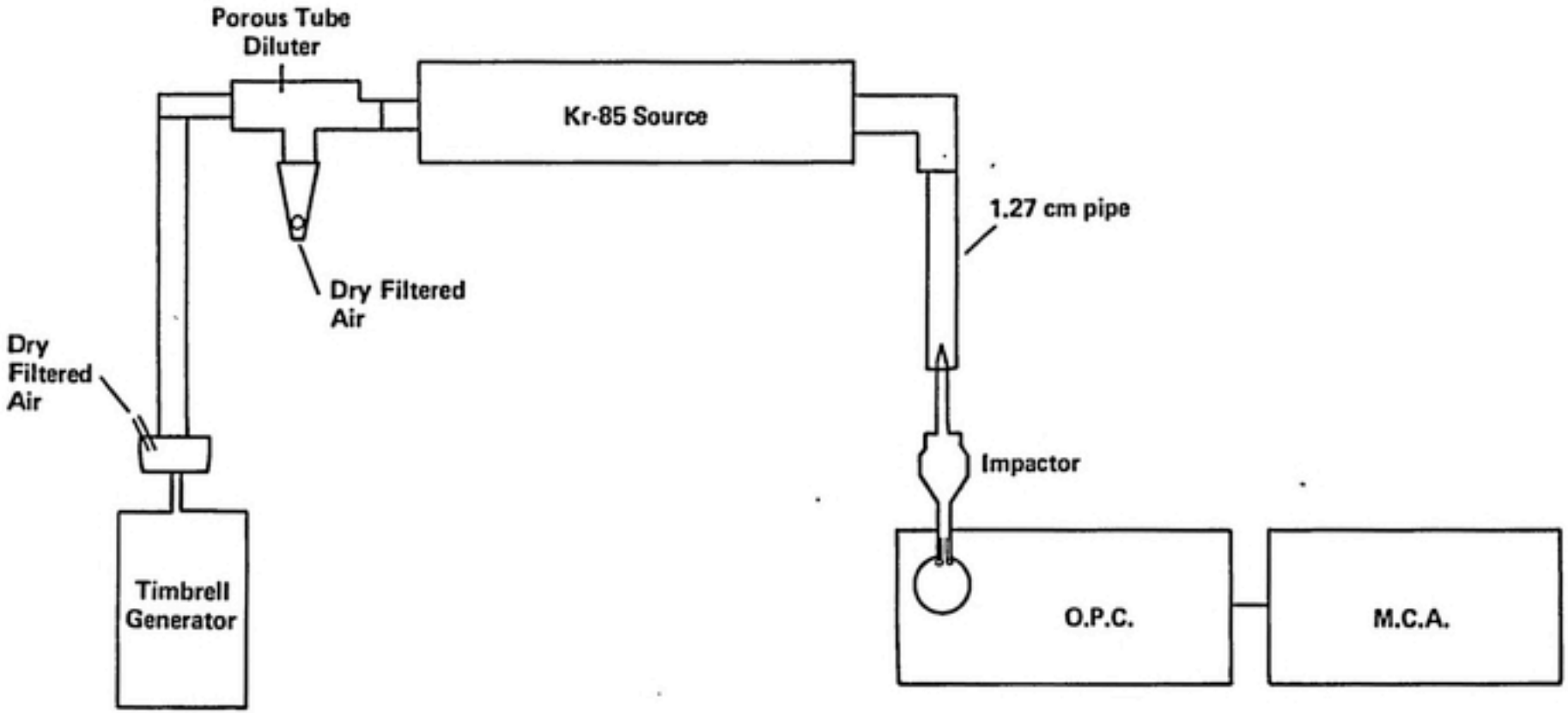

Figure 3-2. Experimental configuration using Timbrell glass bead generator.

The challenge concentration was determined by removing the impaction stage and counting the number of particles penetrating the unobstructed "shell" of the impactor. Collection efficiencies were calculated using the following formula:

$$\eta = \left[1 - \left(\frac{\text{number of particles penetrating impactor}}{\text{number of particles penetrating "shell"}}\right)\right] \times 100 \ .$$

Bounce or rebound is defined as the difference between the collection efficiency of liquid particles and the collection efficiency for a given test aerosol having the same aerodynamic equivalent diameter as the liquid particles.

The relative humidity of the sample air stream was monitored during each run and never exceeded 10 percent.

3.2.1 Impactor Design

Industrial hygiene and air pollution uses of inertial impactors usually require the separation of particles capable of penetrating into the lung, from larger airborne particles. As a generalized case of such a device, the impactor used in this experiment was designed to have a 50-percent collection efficiency for particles having an aerodynamic equivalent diameter of 5 μm.

The simplest possible configuration of an impactor was used to allow the isolation effects due to particle bounce from other factors which might be peculiar to more complex impactor designs. The experimental device was a single-stage impactor with one round jet of 0.47 cm in diameter, operated at a flow rate of 7100 cc/min, drawn by the OPC pump. The jet velocity and Reynolds number were 682.1 cm/s and 2125, respectively. The nozzle was constructed of brass tube; the main body of the impactor was made of aluminum, and the impactor stage was made of stainless steel. The design criteria recommended by Marple and Willeke (1976) were used. Figure 3-3 shows the theoretical characteristic curve of this impactor.

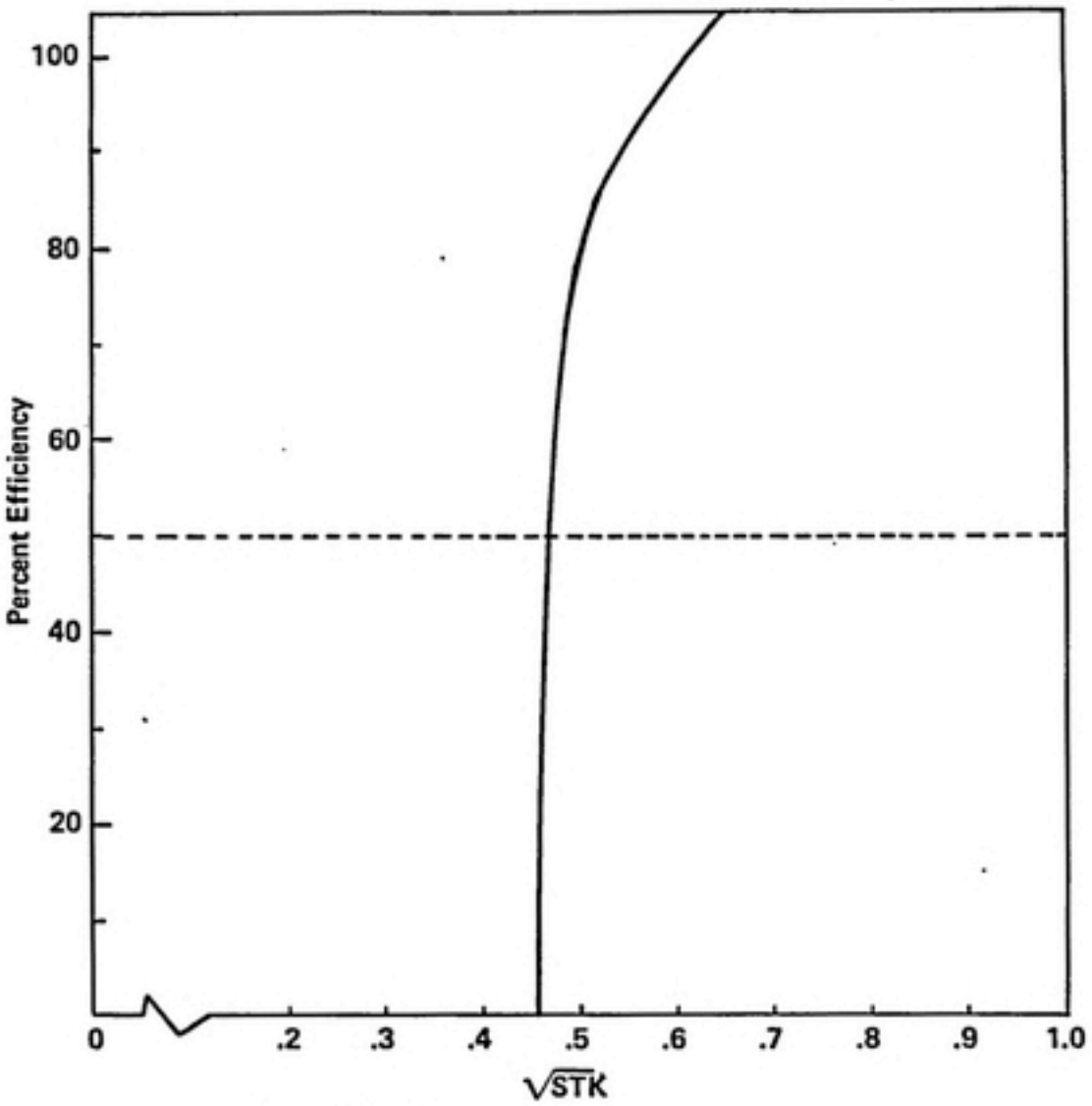

Impactor Theoretical Parameters

D_j = 0.47 cm	Re_j = 2115.8
S/D_j = 2.0	D_{50} = 5.0 μm
V_j = 682 cm/s	Q = 7100 cc/min
$\sqrt{STK}_{50}$ = 0.48	

From Marple and Willeke, 1976

Figure 3-3. Theoretical characteristic curve of experimental impactor.

The nozzle of the impactor was 6.2 cm long beginning with a 7-degree externally tapered section. The internal diameter was 0.47 cm its entire length to the jet exit. All samples were drawn from the centerline of an open duct connected to the generation system (Figure 3-1). The jet exit was 0.94 cm from the impaction surface, giving a jet-to-plate ratio of 2.

Figure 3-4 diagrams the impactor showing the removable stage. Stainless steel and Teflon® substrates were polished to remove any obvious surface imperfections. All substrates were washed in acetone and allowed to dry on a clean Kimwipe between samples.

3.2.2 Particle Generation

Monodisperse ammonium fluorescein and oleic acid-uranine particles were generated using a TSI Model 3450 Vibrating Orifice Aeorosol Generator (VOAG). Particle diameter was determined from particle solution concentrations and VOAG operating parameters (Liu et al., 1974) and were verified by collecting a sample of the aerosol on a treated glass slide and measuring particle diameters with a traveling hair eyepiece calibrated against a stage micrometer. Correction for particle spread was applied to liquid particles according to the method described by Liu et al., (1972). Glass beads were separated with a Donaldson Accucut aerodynamic particle separator (Majack Company) to the desired size fraction. The glass bead feedstock was Potter Industries (Hasbruck, New Jersey) 5000 Series glass beads. Operating conditions selected for the operation of the Donaldson Accucut were designed to produce a fine size fraction consisting exclusively of particles less than 20 μm aerodynamic diameter (ρ glass 2.65 g/cc). A New Porton eyepiece graticule calibrated with a stage micrometer was used to size the fine fraction of the separated beads. A sample of glass beads was collected from the aerosol stream to check for evidence of glass bead breakage using an optical microscope. In addition, the Pyrex collector particle load was viewed under the microscope to assess particle distribution on the collector plate and the level of particle loading. Glass bead samples collected on the Pyrex impactor substrate were also sized and average number of particles per field area were

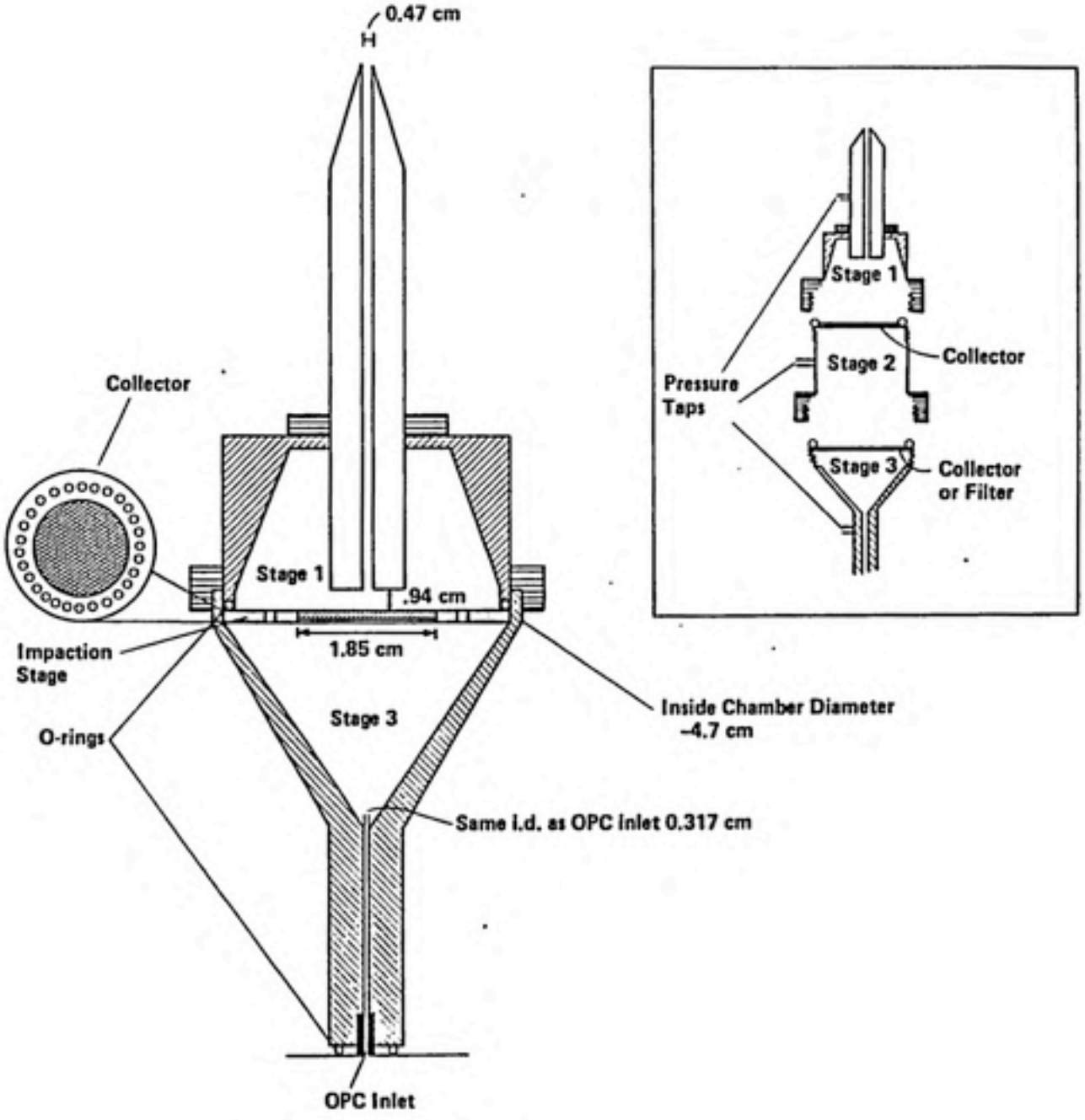

Figure 3-4. Impactor design.

calculated to monitor particle loading. A summary of particle generation methods is provided in Table 3-1.

For this experiment, a glass bead generator capable of delivering airborne beads at a constant concentration for a minimum period of two continuous hours without altering the size distribution of the powder was necessary. A variety of generation techniques were found to be inadequate to this task including a fluidized bed and a brush-based generator. A system based on the asbestos generator described by Timbrell et al. (1968) was tested for compliance with the necessary performance criteria and met performance requirements in all tests. The Timbrell generator performance testing procedures and results are given in Appendix B. Figure 3-5 is a diagram of the glass bead generator.

3.2.3 Particle Detection

Particles were detected with a Climet 210 Optical Particle Counter in conjunction with a Climet 225 Multichannel Analyzer. Background counts were subtracted from challenge and sample counts. In the channels of interest, the background levels accounted for an average of less than 2 percent of challenge counts.

For ammonium fluorescein particles which are dark red-brown in color, it was expected that excessive light absorption combined with fluorescence might pose difficulties in a light-scattering-based detection system. In calibration of the OPC with monodisperse ammonium fluorescein particles using a Tracor Northern Model TN-1705 Pulse Height Analyzer for signal analysis, considerable spread was noted in the signal voltage peak. In addition, the peak appeared in channels corresponding to about half the voltage expected, based on the PSL calibration curves for a 10-μm particle offered by the manufacturer. To ensure that the OPC count results could be reliably used, OPC counts were compared to fluorometry measurements of filter collected samples of the same aerosol.

A series of 14.3-liter samples were taken with the impactor shell in the three-stage configuration. Filter samples were collected by placing 4.7-cm glass-fiber type A-E Gelman filters on the support on the last stage of the impactor with and without the collector in place.

TABLE 3-1. PARTICLE GENERATION METHODS

Particle Material	Raw Feed	Bulk Density (g/cc)	Diameter (μm) Aerodynamic	Physical	Generator	Operating Conditions	Reference	Particle Diameter Verification
Oleic Acid - Uranine	oleic acid and uranine dissolved in methanol	0.8935	3.0 5.0 7.0 10.0	3.2 5.3 7.4 10.6	TSI Model 3045 Vibrating Orifice Aerosol Generator	Dilution Air: 23000 cc/min Dispersion Air: 1500 cc/min Downstream Dilution Air: 27336 cc/min	TSI Manual Berglund & Liu (1973)	1) VOAG parameters 2) Collection on 2% Nyebar coated slides sized with stage micrometer traveling hair eypiece; optical microscope (Olan et al., 1982)
Ammonium Fluorescein	fluorescein dissolved in 0.1N NH_4OH	1.35	3.0 5.0 7.0 10.0	2.6 4.3 6.0 8.6	Same as above	Same as above	Vanderpool (1984)	1) VOAG parameters 2) Collection on glass slide sized with micrometer calibrated traveling hair eyepiece
Glass Beads	Potter Industries Series 5000 glass beads	2.65	Polydisperse Range 0.5-15 μm cmad: 3 μm		Modified Timbrell	Supply Air: 40000 cc/min Downstream Dilution Air: 3000 cc/min	Timbrell et al. (1968)	1) Donaldson Accucut, Majack Co., with cutpoint < 20 μm aerodynamic diam. 2) Optical microscopy using New Porton graticule sizing; minimum 100 field or 100 particles 3) Climet CI-225 OPC and Climet CI-210 Multichannel Analyzer

*Covered in detail in Appendix A.

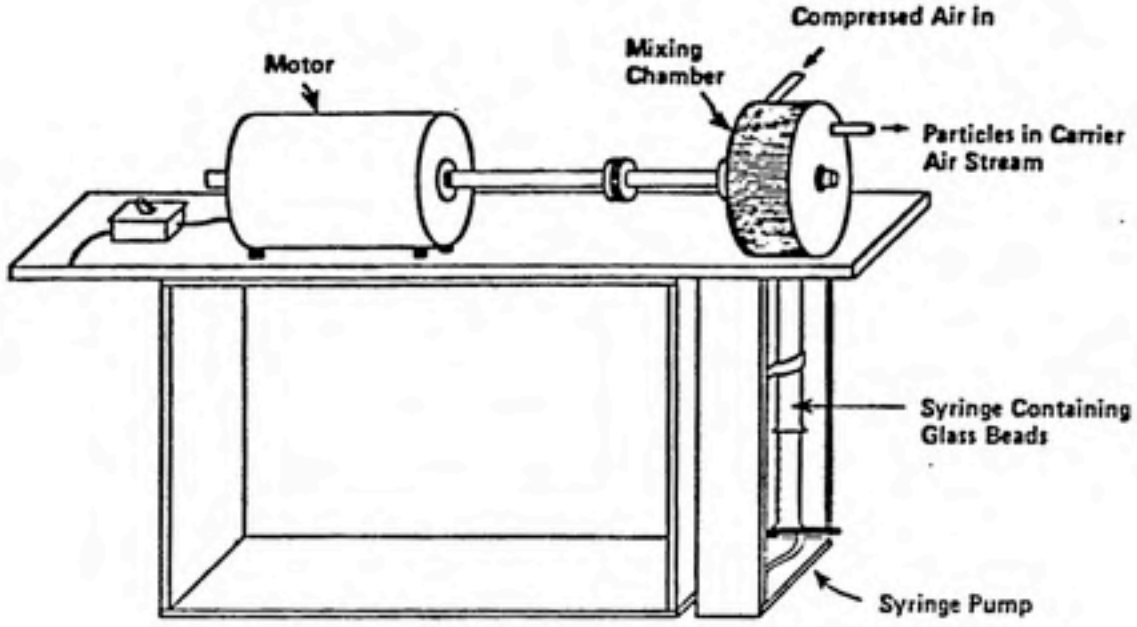

View 1: Generator in normal operating configuration.

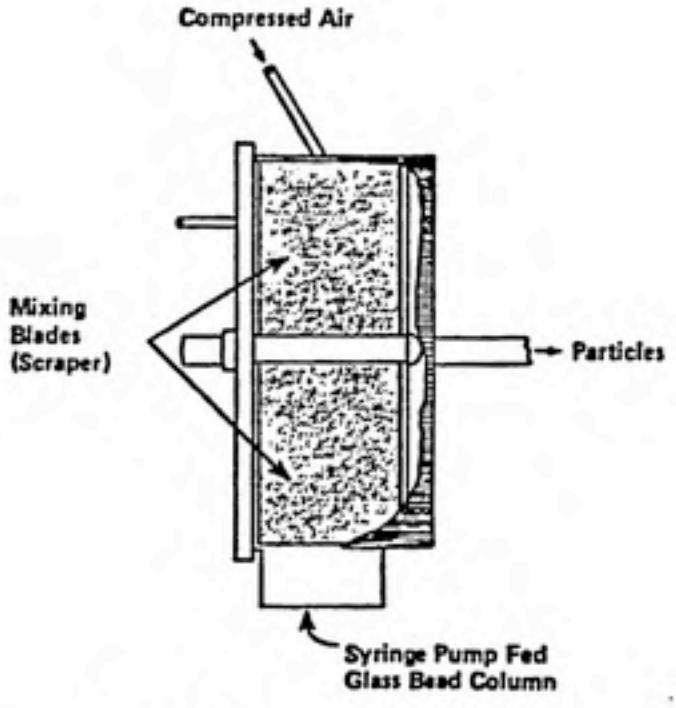

View 2: Cross section of mixing chamber.

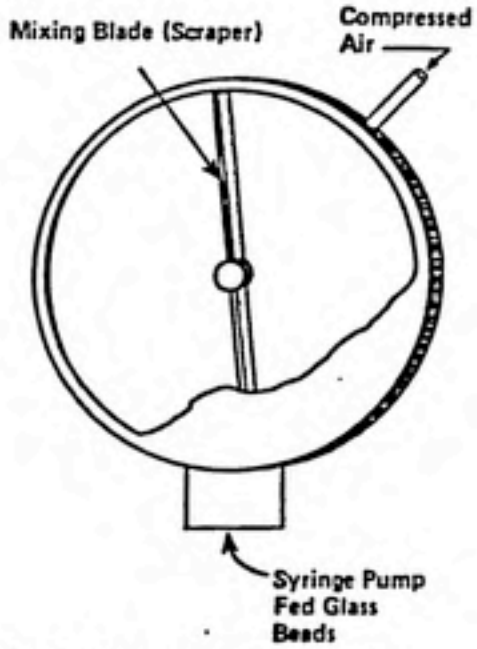

View 3: Cut away of mixing chamber.

Figure 3-5. Glass bead generator based on the design of Timbrell et al. (1968).

Those were alternated with samples counted by the OPC with no filter in place.

The filters were desorbed in a 0.1-N solution of ammonium hydroxide, and an aliquot was analyzed in a Turner Model 112 Fluorometer. The fluorescence reading was converted to mass from comparison with a fluorometer calibration curve generated using successive dilutions of the 10-μm ammonium fluorescein particle solution. This mass reading was converted to count by dividing the total mass collected by the mass of one 10-μm particle. Agreement between the OPC determined collection efficiency and fluorometry results was within 5.0 percent.

4.0 RESULTS AND DISCUSSION

4.1 Estimation of Error

Estimation of errors was calculated using a method developed by Kashdan (1984), specifically for the comparison of impactor data. Standard deviation of the collection efficiency ratio estimate, R* was calculated with:

$$\text{Std Dev } (\hat{R}) = \hat{R} \sqrt{\frac{1}{n}\left((CV{:}N_o)^2 + (CV{:}\text{sample})^2 - \frac{Cov}{100}\right)} \quad , \quad (10)$$

where relative covariance, Cov, is calculated as:

$$Cov = \frac{1}{n-1} \Sigma\, N_o \bullet \text{sample} - \frac{\Sigma\, N_o \bullet \Sigma\, \text{sample}}{n} \quad , \quad (11)$$

and n is the number of replicate samples, N_o is the number of particles penetrating the impactor when all collisions with the substrate result in particle capture, and CV is the ratio of the standard deviation of the replicates to their mean.

4.2 Collection Efficiencies

Results of the studies of collection efficiencies are plotted in Figures 4-1 to 4-6, and Table 4-1 lists the estimate of collection efficiency. Figure 4-1 shows the calibration curve generated using oleic acid-uranine particles with the theoretical impactor curve and that determined with polydisperse glass beads on an oiled glass frit. The two experimental curves show close agreement and similar slopes. The glass frit curve shows a maximum collection efficiency of 92 percent with an uncertainty of 8.84 percent at the 90-percent confidence level using a students t-test, showing good agreement with the findings of Hering (1984). Both curves indicate an impactor cut-point of approximately 5.3 μm which is close to the design point of 5 μm. The two experimental curves show considerably shallower cut characteristics than would be expected based on the ideal curve for the

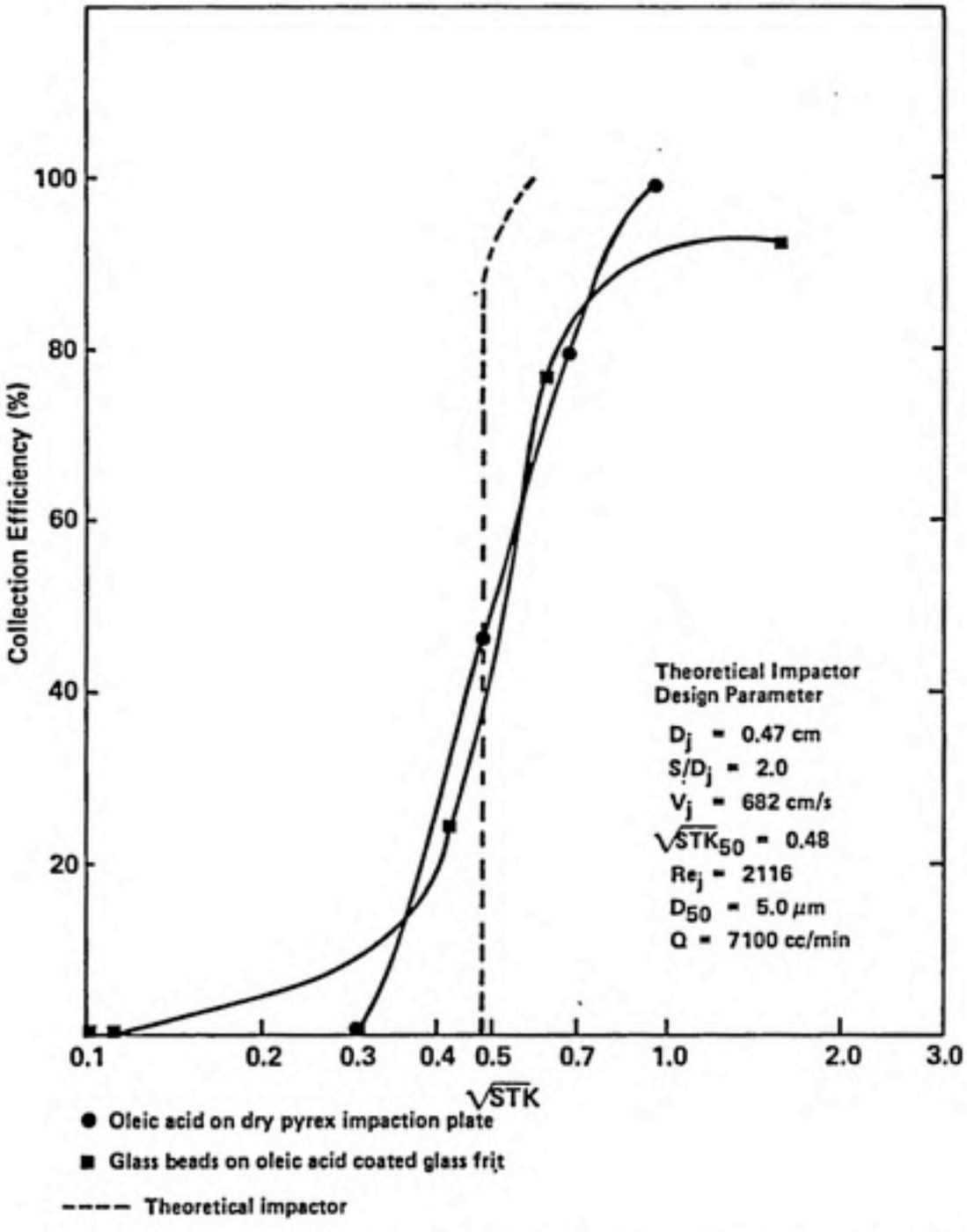

Figure 4-1. Comparison of calibration curves for the experimental impactor generated with oleic acid-uranine particles on a pyrex collector and glass beads on an oleic acid-soaked glass frit, with the theoretical collection efficiency curve.

impactor. This is likely due to the formation of nonideal flow patterns in the impactor chamber immediately above the impaction plate. The ideal impactor has no such chamber, and the jet plate runs infinitely parallel to the impaction plate plane in the models (Marple, 1970).

Figure 4-2 shows the effect of changing the collector material on the collection efficiency of ammonium fluorescein particles. Based upon the significance of collection efficiency differences at the 90-percent confidence limit, onset of bounce occurs between 3 and 5 μm on all three collector materials, with no significant difference at 7 μm with the stainless steel collector surfaces. A comparison of the peak collection efficiency for the three surfaces shows a significant difference between all three materials. At 10 μm, however, there is no significant difference between the collector materials.

The apparently anomalous reduction in bounce at 7 μm on the stainless steel surface may be related to the size, shape, and spacing of surface irregularities. Surface irregularities have been reported by Corn and Stein (1978) to increase collection efficiency.

The relative bounciness of Pyrex and stainless steel seem to correspond to relative hardness in agreement with the findings of Esmen (1975) with brass and aluminium collectors discussed in the literature review. However, Teflon® is clearly a softer material than either of the other two materials. Hering (1984) reported similar results when comparing dry glass impaction surfaces with a 10-μm pore Teflon® Membrana filter with test aerosols of PSL spheres. The dry glass tests reached a maximum collection efficiency at over 60 percent while the Teflon® filter maximum was less than 40 percent. The two materials showed the same collection efficiency at a $\sqrt{Stk}$ of approximately 0.6, corresponding to a collection efficiency of near 18 percent.

The strong fluorocarbon bonding in Teflon® appears to be a greater determinant in the particle-collector interaction than is the relative hardness of the materials.

Figure 4-3 compares the relative bounce of glass beads on the three collector surfaces. Most striking in this figure is the "over collection" of glass bead particles below a $\sqrt{Stk}$ of 0.6. The difference between the collection efficiencies for all three collector

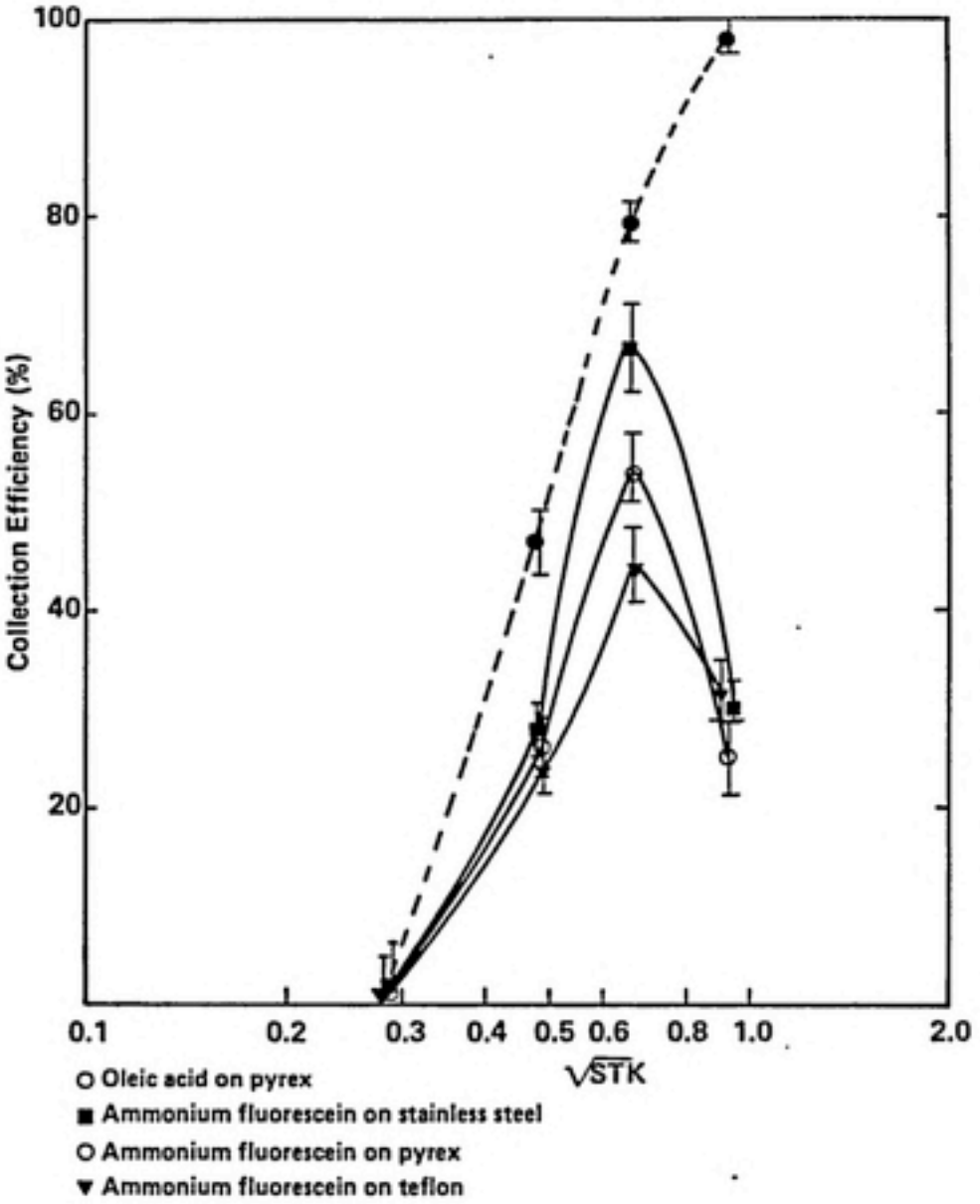

Figure 4-2. Ammonium fluorescein and oleic acid collection efficiencies on three collector materials.

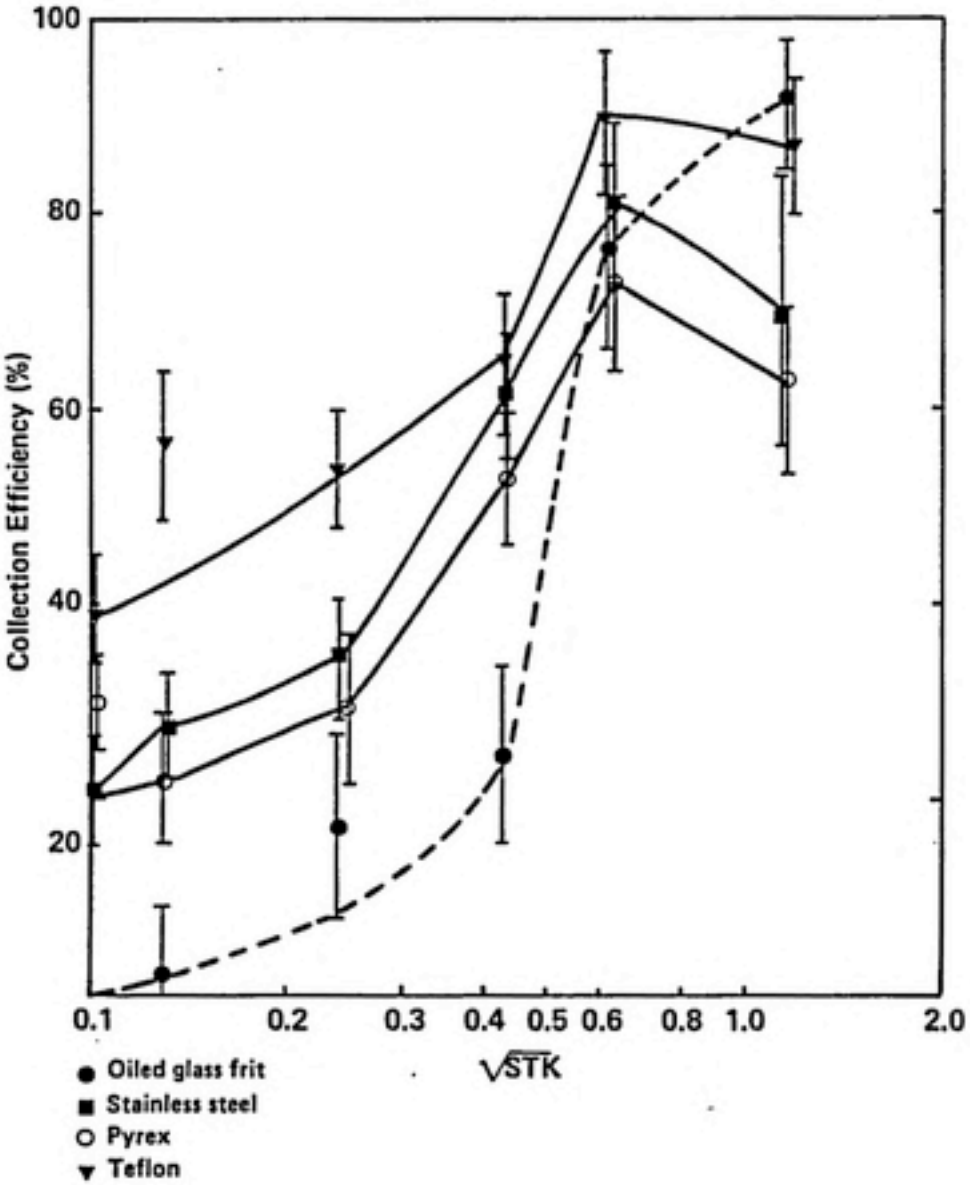

Figure 4-3. Glass bead collection efficiencies on four collector materials.

materials is significant at the 90-percent confidence level. The difference between Pyrex and stainless steel is not significant at any point along the respective curves. There is, however, a significant difference between the points for stainless steel and Pyrex from those for Teflon®.

The glass bead data was collected in two different sampling regimes. Small volume 2.84-liter samples were taken with four replicates for each collector in random order in the first experiment. In the second experiment, one 142-liter sample was taken for each substrate in random order. The large volume sample was monitored at 1-liter intervals so that 142 consecutive 1-liter samples were drawn for each substrate and for the impactor shell with no substrate in place. A smaller sample consisting of 10 consecutive 1-liter counts was selected randomly from the series of 142 samples. The means of both sample types are reported in Table 4-1. The data in the figures consists of averages of ten consecutive 1-liter samples. Agreement between the two sample types was well within the experimental error.

The Pyrex collector was examined microscopically to determine the size distribution of the collected particles.

Table 4-2. Comparison of Microscopy and OPC Results Glass Bead Collection on Pyrex Collector

Collection Efficiency - Four-Minute Sample			
d (μm) (mid-range)	Microscopy (%)	OPC (%)	
		oleic acid on Pyrex	glass frit
2.5	28.1	0	5
3.5	13.3	5	13
4.9	21.5	43	39
6.9	98.1	77	82
9.9	100.0	98	92

Table 4-2 shows the ratio of glass beads collected on the substrate as a ratio to the number of glass beads in that size interval which were found in the raw feed material. The other two columns show the collision efficiency of oleic acid-uranine particles and glass

TABLE 4-1. EXPERIMENTAL RESULTS, COLLECTION EFFICIENCY, ADHESION PROBABILITY

Particle Material	Collector Material	d (μm) Aerodynamic	$\sqrt{Stk}$	η	h	Number of Samples
Ammonium Fluorescein	Stainless Steel	3.0	0.29	0.009±0.029	1.00	4
		5.0	0.48	0.28±0.032	0.68	4
		7.0	0.67	0.67±0.016	0.86	4
		10.0	0.95	0.30±0.107	0.30	4
	Pyrex	3.0	0.29	0.003±0.043	1.00	4
		5.0	0.48	0.26±0.012	0.57	4
		7.0	0.67	0.54±0.0344	0.68	4
		10.0	0.95	0.25±0.0312	0.26	4
	Teflon	3.0	0.29	0.006±0.019	--	4
		5.0	0.48	0.23±0.014	0.55	4
		7.0	0.67	0.44±0.038	0.63	4
		10.0	0.95	0.33±0.031	0.33	4
	Oiled Glass Frit	7.0	0.67	0.78±0.021	--	5
Oleic Acid/ Uranine (Liquid)	Stainless Steel	3.0	0.29	0.02±0.046	--	4
		5.0	0.48	0.41±0.038	--	4
		7.0	0.67	0.78±0.016	--	4
		10.0	0.95	0.99±0.011	--	4
	Pyrex	3.0	0.29	-0.01±0.002	--	3
		5.0	0.48	0.46±0.025	--	4
		7.0	0.67	0.80±0.034	--	3
		10.0	0.95	0.98±0.039	--	4
	Teflon	3.0	0.29	--	--	--
		5.0	0.48	0.42±0.037	--	4
		7.0	0.67	0.70±0.004	--	4
		10.0	0.95	0.99±0.012	--	4

(continue)

TABLE 4-1 (continue)

Particle Material	Collector Material	d (μm) Aerodynamic	$\sqrt{Stk}$	η	h	Number of Samples
		(median diameter in Climet 225 size ranges)				
Glass Microspheres	Oiled Glass	0.9	0.10	0±0.075	--	10
	Frit	1.4	0.14	0.02±0.102	--	10
		2.5	0.24	0.12±0.084	--	10
		4.5	0.43	0.25±0.090	--	10
		6.5	0.62	0.77±0.069	--	10
		12.2	1.16	0.92±0.0150	--	10
	Stainless Steel	0.9	0.10	(0.18)0.21*±0.048	--	(4)10
		1.4	0.14	(0.20)0.28±0.049	14.00	(4)10
		2.5	0.24	(0.32)0.35±0.047	2.92	(4)10
		4.5	0.43	(0.55)0.61±0.045	0.40	(4)10
		6.5	0.62	(0.80)0.81±0.071	1.05	(4)10
		12.2	1.16	(0.73)0.69±0.146	0.75	(4)10
	Pyrex	0.9	0.10	(0.16)0.29±0.044	--	(4)10
		1.4	0.14	(0.22)0.21±0.065	10.50	(4)10
		2.5	0.24	(0.33)0.30±0.064	2.50	(4)10
		4.5	0.43	(0.50)0.54±0.054	2.16	(4)10
		6.5	0.62	(0.78)0.72±0.082	0.94	(4)10
		12.2	1.16	(0.42)0.62±0.071	0.67	(4)10
	Teflon	0.9	0.10	0.40±0.051	--	4
		1.4	0.14	0.56±0.043	28.00	4
		2.5	0.24	0.54±0.044	4.50	4
		4.5	0.43	0.64±0.041	2.56	4
		6.5	0.62	0.90±0.062	1.17	4
		12.2	1.16	0.87±0.082	0.95	4

Values reported in parenthesis () are for short duration samples.

*Values reported in this column are for ten 1-minute consecutive samples selected randomly from a larger sample.

beads on an oiled glass frit substrate as determined with the OPC and taken from the calibration curves for the impactor. An unexpectedly high count of glass bead with an aerodynamic diameter of less than 2.5 μm (mid-range of the sizing interval) appear on the glass plate when examined under the microscope. It should be noted that microscopic sizing of particles collected on the glass plate was performed in the case of only one 4-minute sample of glass beads. Further, comparison of microscope counts of the oleic acid-uranine particles and OPC collected data was not undertaken as part of this study. However, the comparisons presented in Table 4-2 do tend to support the increase in collision efficiency noticable in the OPC collected data when glass beads are used with any of the collector substrates.

A similar over collection of low Stokes number particles was present in data reported by Rao and Whitby (1978). Using PSL particles on glass fiber filters, Whatman filters, and dry glass collection surfaces in two different impactors, collection efficiencies for $\sqrt{Stk}$ less than approximately 0.48 were higher for the listed substrates than for an oiled glass surface. The detection method used in this study was optical particle counting with a Royco 220 OPC. Loeffler (1974) also noted a similar increase in collision efficiency when testing polyamide fibers with glass beads, quartz particles, and paraffin particles. He concluded that electrostatic forces make a large contribution to particle transport processes as the particles approach the fiber. In a subsequent study, Loeffler (1977) modeled the collection of particles by a single fiber with and without taking into account electrostatic forces. Model curves of collection efficiency versus Stokes number showed that particles with small Stokes numbers are collected very efficiently. The collection efficiency due to inertia, gravity, and electrostatic forces reaches a maximum at a Stokes number near zero. The collection efficiency then drops off to a minimum near a Stokes number of 1. When electrostatic forces are not included in the model, the curve is more or less flat at a much smaller collection efficiency until a Stokes number of 1 is reached, and then collection efficiency rises steeply with increasing Stokes numbers.

All of these experimental studies, including the current study, used some means to neutralize the charge on the particles. The

collector is grounded through its metal base. In the present study, the activity of the neutralizer was monitored before and after the experiment and found to be about 80 percent of the full 10 mCi activity level corresponding to a reasonable decay rate given the half-life of Kr-85. The total air volume through the neutralizer was less than 50 l/min, well below the neutralizer's recommended capacity of 150 l/min.

Contact charging, either by pure contact or by triboelectrification due to friction may be responsible for the increase in collision efficiency of smaller glass beads. If contact charging were taking place, it would be more likely to appear with a polydisperse aerosol. In monodisperse suspensions of small particles, inertial forces do not bring any particles in contact with the collection surface. However, with a polydisperse suspension, large particles would hit the plate, giving an opportunity for charge to transfer to the plate. The charge buildup on the plate would preferentially draw small particles to the surface when they came in the vicinity of the charged collection plate. In addition, particles which would not be collected by the mechanism of impaction travel in a path nearly parallel to the impaction plate with relatively high radial velocities and small vertical velocities until the air stream passes through the holes in the impaction plate. This passage of the particle near the plate with some potential for friction to occur, particularly with collected particles resting above the collector surface, might enhance triboelectric effects. (Glass is generally placed at the extreme positive end of a triboelectric series, while Teflon® is usually at the extreme negative end.) This would be consistent with the Teflon® going from being the bounciest of the surfaces with ammonium fluorescein particles to being the least bouncy surface with glass particles.

Figures 4-4 to 4-6 compare the collection efficiency of the two particle materials. Ammonium fluorescein is clearly the bounciest particle material on all surfaces.

Figure 4-7 shows a log-log plot of particle adhesion probability (as defined on Page 5) for ammonium fluorescein versus the kinetic energy of the particle normal to the collector at the point of impact. The kinetic energy was calculated from impact velocities normal to the plate at point of impact estimated from Marple's model as shown in

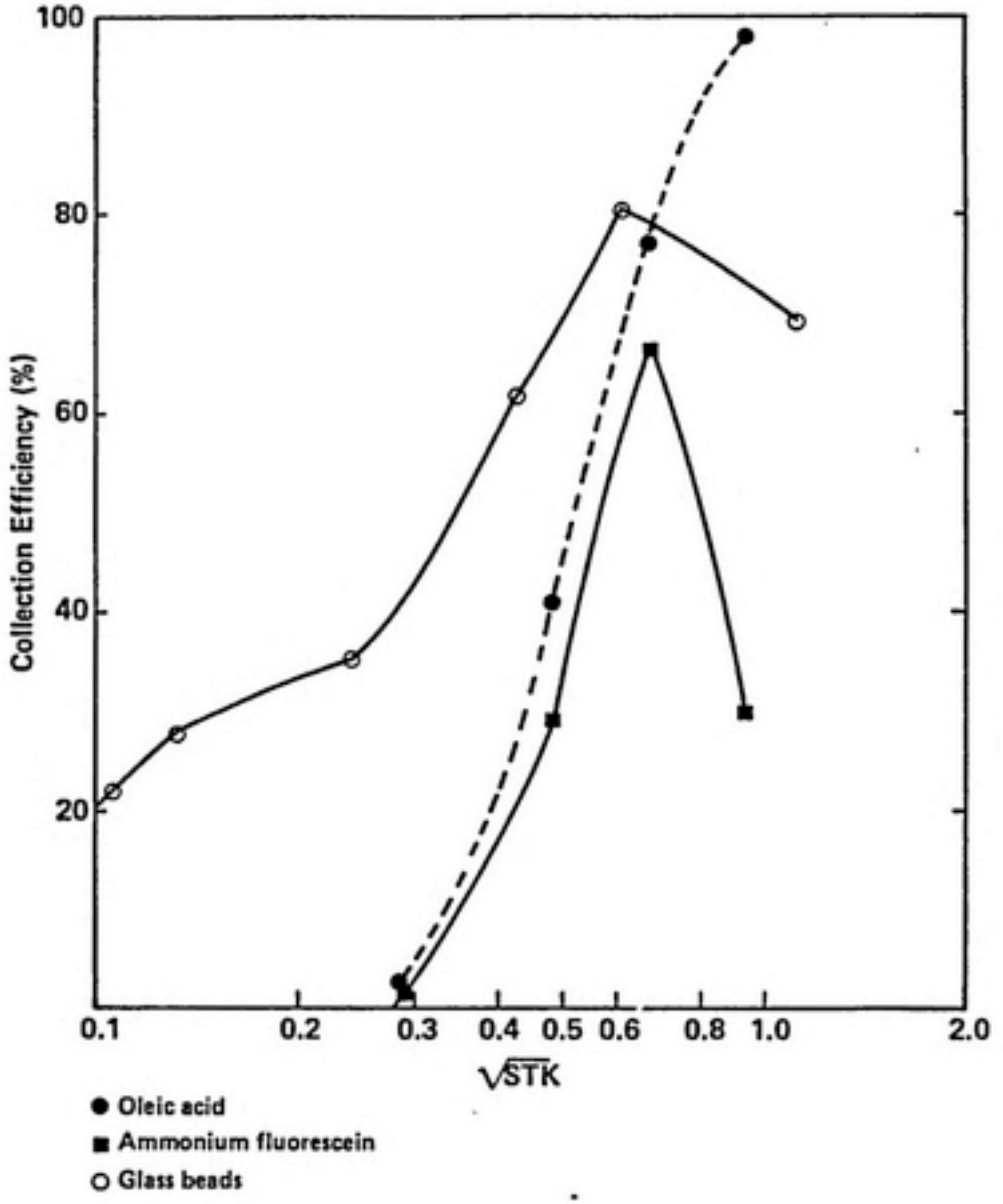

Figure 4-4. Collection efficiencies of glass beads, ammonium fluorescein and oleic acid on a stainless steel collector.

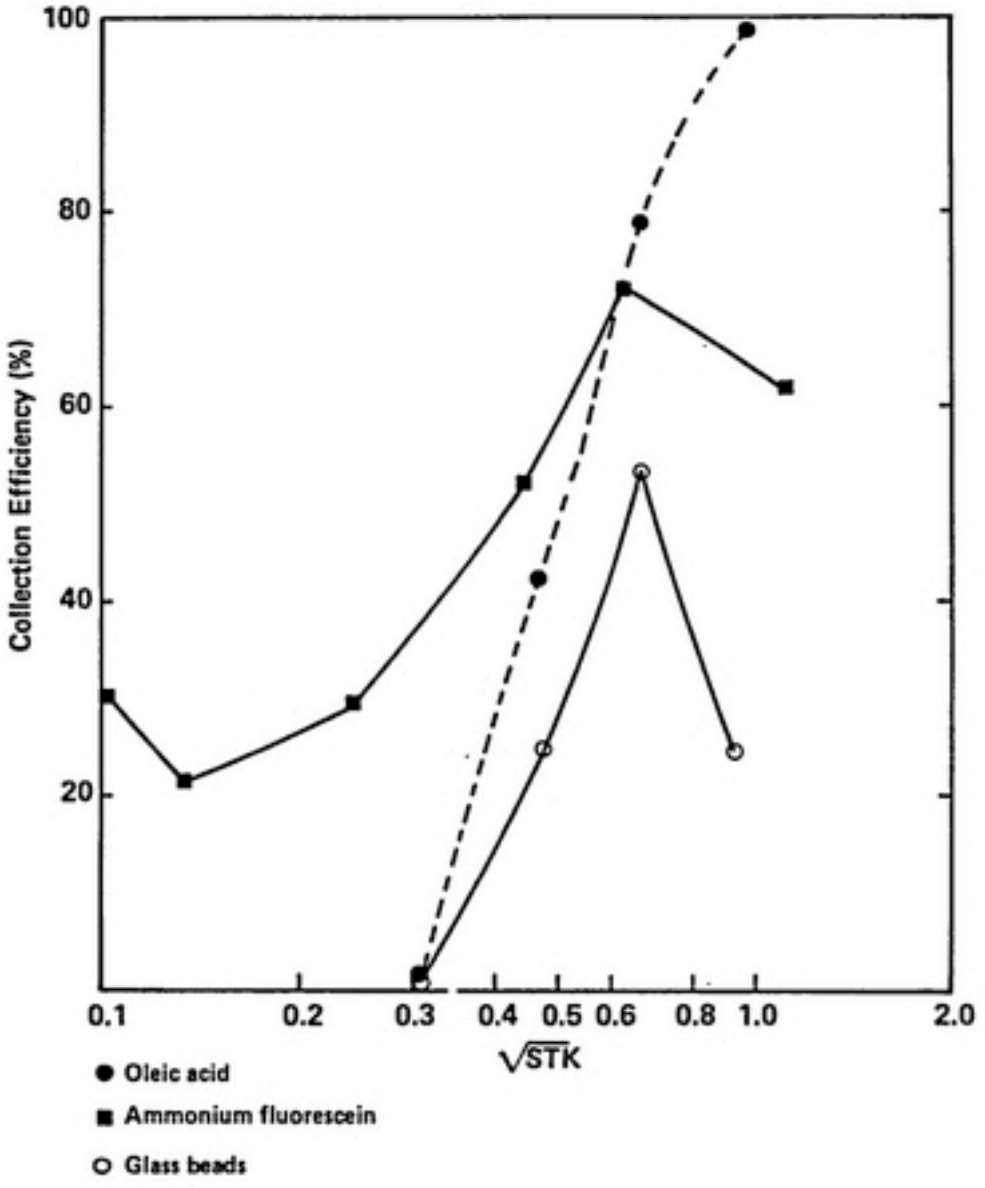

Figure 4-5. Collection efficiencies of glass beads, ammonium fluorescein and oleic acid on a pyrex collector.

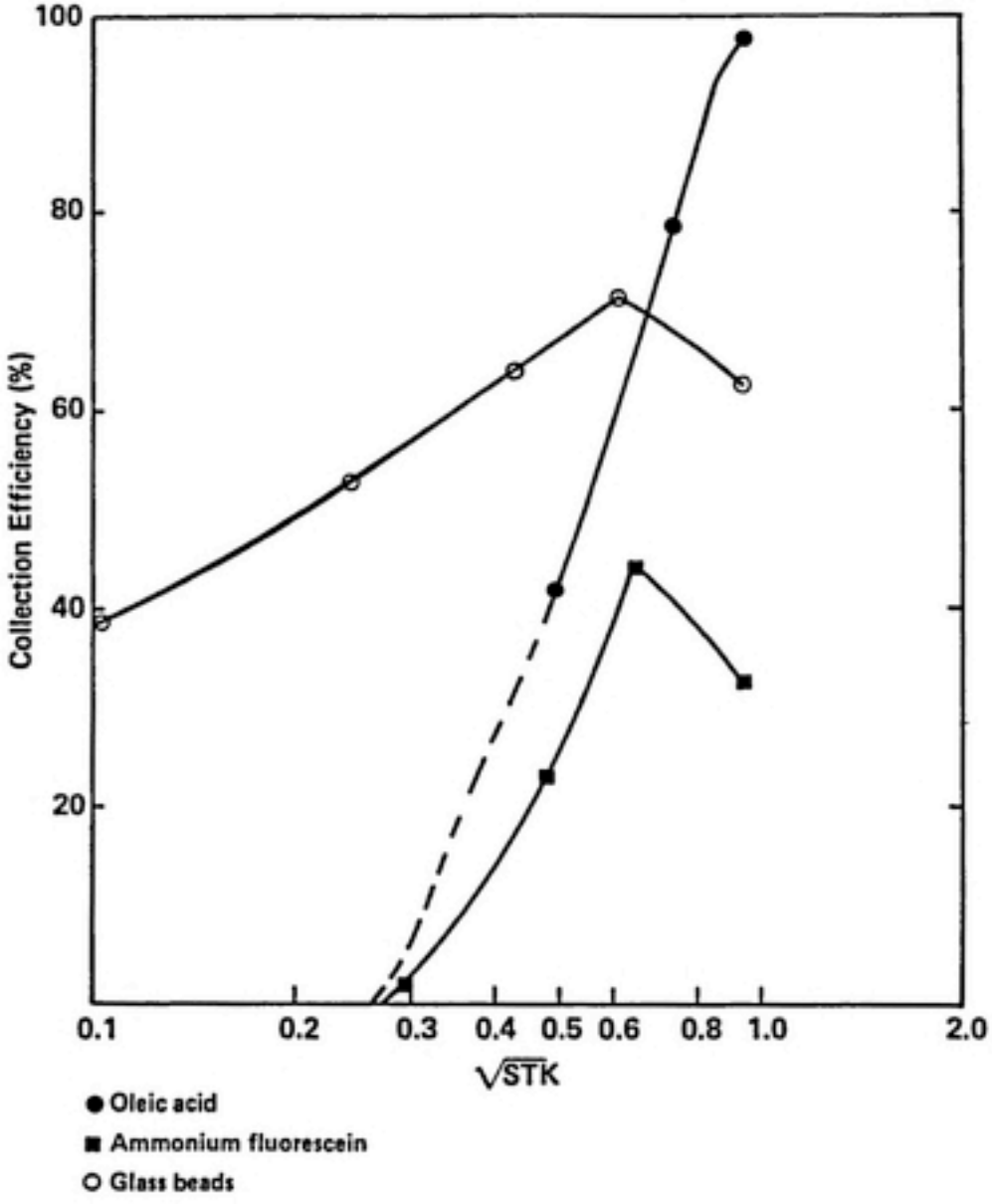

Figure 4-6. Collection efficiencies of glass beads, ammonium fluorescein, and oleic acid on a teflon collector.

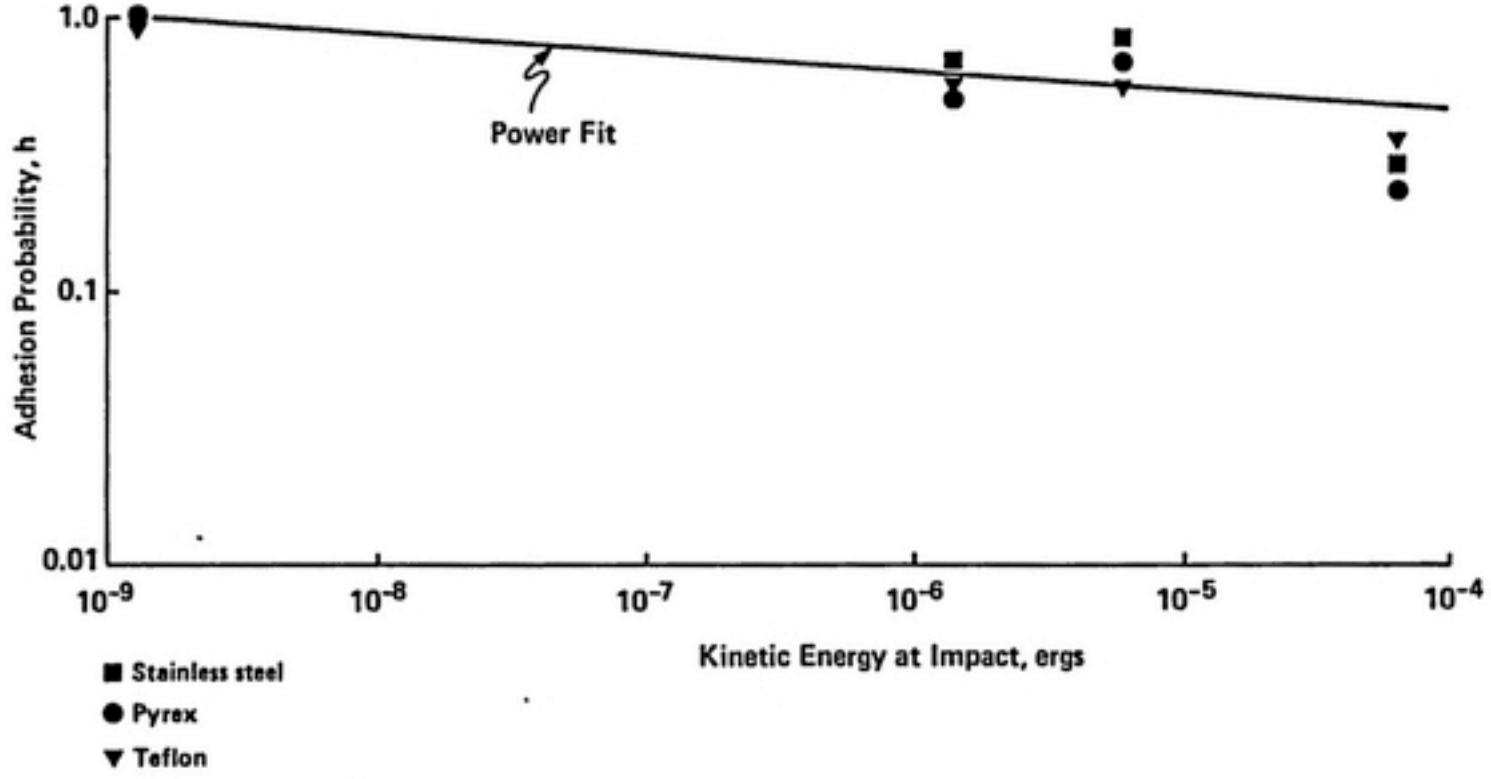

Figure 4-7. Adhesion vs. energy at impact for ammonium fluorescein particles on stainless steel, pyrex and teflon collectors.

Figure 2-1. The data fits a power fit relatively well with a correlation coefficient of 0.71. However, with so few data points, it is difficult to draw conclusions from the fit. Figure 4-8 shows the ammonium fluorescein on stainless steel data with other literature reported values for metal substrates. The data agrees well with that reported by Esmen et al. (1977), who used uranine particles on brass and aluminum collectors. The third set of data points are for fly ash particles on stainless steel fiber mats. The irregular shape of the fly ash may be responsible for some of the variation in this curve.

By projecting the power fit back to 100-percent adhesion probability, an estimate can be made for the kinetic energy of the particle at impact where no bounce occurs. From the value for kinetic energy, the V* and the Bradley-Hamaker constant can be calculated for ammonium fluorescein. The critical kinetic energy based on the power fit is 1.5×10^{-9} ergs, which gives a V* of 14.6 cm/s and a Bradley-Hamaker constant of 2.4×10^{-12} ergs for a unit density 3-μm particle. Both these values agree well with the theory and with literature reported values for similar experiments and are listed in Tables 2-1 and 2-2.

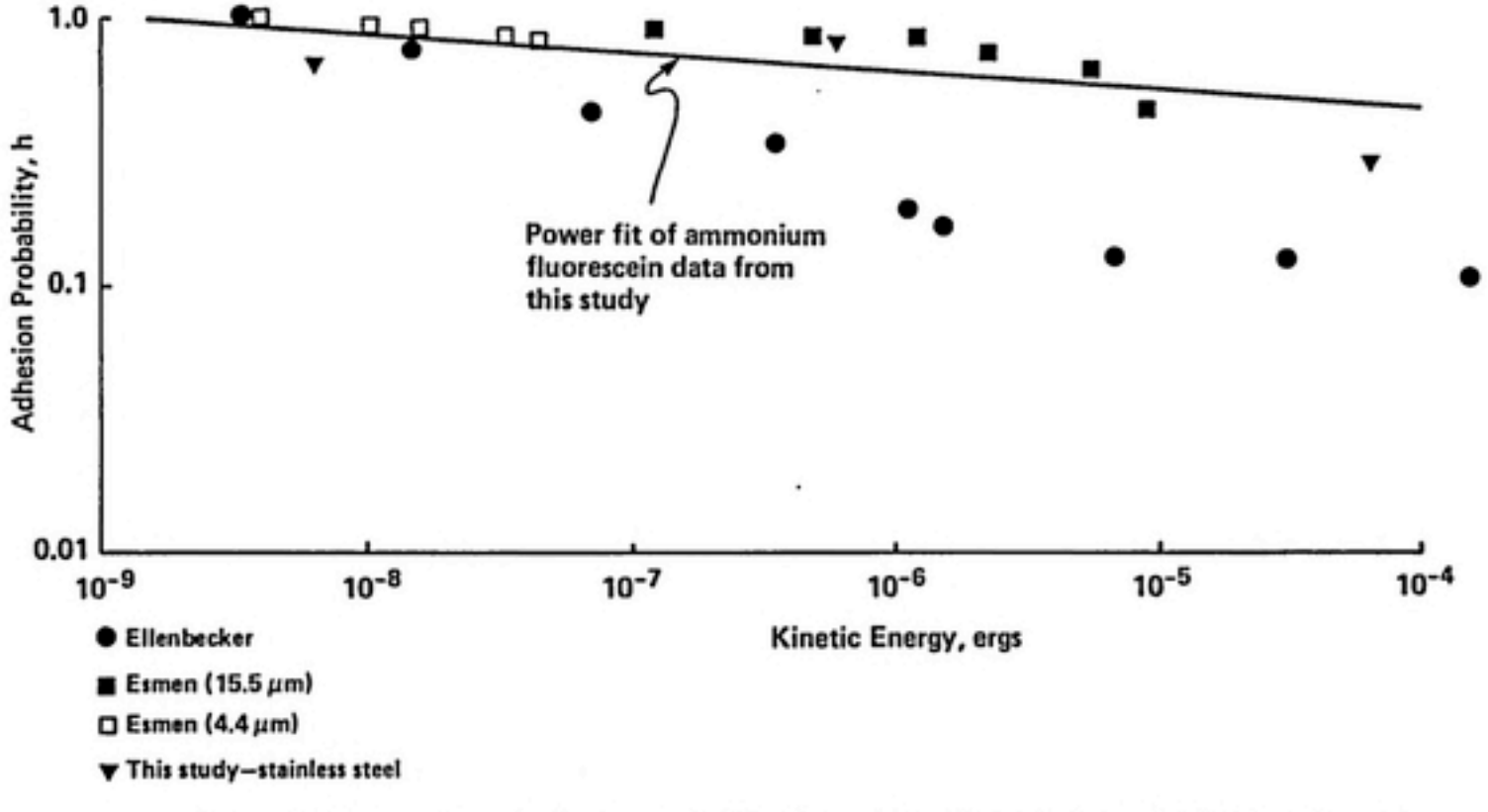

Figure 4-8. Comparison of adhesion probability from this study with those of other investigators.

5.0 CONCLUSIONS AND RECOMMENDATIONS

A study of particle bounce in a laboratory constructed impactor using two particle materials and three different collector substrates has been undertaken. The experimental results, using ammonium fluorescein particles and substrates of polished stainless steel and Pyrex, show good agreement with literature reported values for similar experiments. Based the results of this study and of similar studies reviewed, the following conclusion are drawn:

1. A rudimentary relative scale of substrate bounciness might be based upon the hardness of the collector material. Relative bounciness for metal substrates and glass correspond well with the Mohs hardness scale, for instance. However, a polished Teflon® collector used in this study was found to cause more particle rebound than either of the other two harder surfaces. This result was supported by the only other study found which used Teflon® substrates.

2. On the basis of experimental results with polydisperse glass beads, transport mechanisms in addition to inertial forces may be necessary to fully account for particle collision with the plate. One mechanism proposed is that of contact charging of the plate in the presence of a suitable polydisperse aerosol.

3. Calculations of critical velocity for onset of bounce and the Bradley-Hamaker constant for the materials from the experimental results were made according to the theory proposed by Dahneke (1971). These estimated values agreed well with independantly reported values, tending to support the theory.

Based on the findings, the following recommendations are made:

1. These experiments should be repeated with soft materials other than Teflon® to test the proposed relative bounce scale which is based on the relative hardness of the materials.

2. Experiments should be conducted using a detection method other than optical particle counting which will confirm whether or not collision efficiency is increased with

dry collectors and glass beads as compared to glass beads on an adhesion coated surface.

3. If a collision efficiency increase is confirmed, experiments should be conducted to determine if and where particle or collector charging is taking place.

REFERENCES

Berglund, R. N., and B. Y. H. Lui, Environmental Science and Technology,Vol. 7, 147, 1973.

Cheng, Y. S. and H. C. Yeh, Environmental Science and Technology, 13,1393, 1979.

Corn, M. and F Stein, American Industrial Hygiene Association Journal, July-August,325, 1965

Dahneke, B., Journal of Colloid and Interface Science, Vol. 37, 342, 1971.

Dahneke, B., Journal of Colloid and Interface Science, Vol. 45, 584, 1973.

Dahneke, B., Journal of Colloid and Interface Science, Vol. 1, 58, 1975.

Davies, C.N., A. Aylward and D. Leacey, Archives of Industrial Hygiene and Occupational Medicine, Vol. 4, 354, 1951.

Ellenbecker, M. J., D. Leith, and J. M. Price, Journal of the Air Pollution Control Association, 30, 1224, 1980.

Esmen, N. A., P. Ziegler, and Robert Whitfield, Aerosol Science, 9,547, 1978

Fuchs, N. A.,"Aerosol Impactors (A Review) ", in Fundamentals of Aerosol Science, ed. D. T. Shaw, John Wiley and Son, New York, 1978.

Goetz, A. A., Environmental Science and Technology, Vol. 3, 154, 1969.

Hering S. V., " Developments in Bounce Free Impaction Surfaces", Final Report, Environmental Protection Agency, Grant No. R808786-01-2, June 1984, (under review).

Hu, J. N. H., Environmental Science and Technology, Vol. 5, 251, 1971.

Hamilton, R. J. , T. Wainwright and W. H. Walton, British Journal of Industrial Medicine, Vol. 8, 14, 1951.

Kashdan, E., personal communication 1984.

REFERENCES (continued)

Liu, B. Y. H. and D. Y. H. Pui, Atmospheric Environment, Vol. 16, 563, 1972.

Loeffler, F., Clean Air, Vol. 8, 1974.

Loeffler, F., "The Influence of Electrostatic Forces for Particle Collection in Fibrous Filters.", in Novel Concepts, Methods and Advanced Technology in Particulate - Gas Separation, ed. T. Ariman, University of Notre Dame, April 20-22, 1977.

Marple, V. A., " A Fundamental Study of Inertial Impactors", Ph.D. dissertation, University of Minnesota, Particle Technology Laboratory Publication No. 144, 1970.

Marple, V. A. and B. Y. H. Liu, Environmental Science and Technology, 8, 648, 1974.

Marple, V.A., Journal of Colloid and Interface Science, 53, 31, 1975.

Marple, V. A. and K. Willeke, Atmospheric Environment, 10, 891, 1976.

Mercer, T. T., and R.G. Stafford, Annuls of Occupational Hygiene, Vol. 12, 41, 1969.

Mercer, T. T. and H. Y. Chow, Journal of Colloid and Interface Science, Vol. 53, 121, 1969.

Paw, U. K. T., Journal of Colloid and Interface Science, Vol. 93, 442, 1983.

Ranz W. E. and J. B. Wong, Archives of Industrial and Occupational Medicine, 5, 464, 1952.

Rao, A. K. and K. T. Whitby, Journal of Aerosol Science, Vol. 9, 77, 1978.

Reischl, G. P., and W. John, Staub Reinhalt Luft, Vol. 38, 55, 1975.

Timbrell, V., A. W. Hyett and J. W. Skidmore, Annuls of Occupational Hygiene, Vol. 11, 273, 1968.

Willeke, K. and J. MacFeeters, Journal of Colloid and Interface Science, Vol. 53, 121, 1975.

Vanderpool, R. W., and K. L. Rubow, TSI Quartley, Vol. X, Issue 1, 1984.

APPENDIX A

Pilot Study

A study was conducted to select materials and methods for the experimental procedures used in the current report. A single-stage round impactor designed to have a cutpoint of 10.0 µm was constructed of stainless steel and brass. The impaction plate of polished stainless steel was removable from the device. The impactor was pressure fitted to a Climet 208 light scattering OPC. The OPC was modified in the following ways:

1. The wiring was modified to allow removal of the optics probe to a distance up to 1.5 m from the instrument frame.

2. The particle size detection range of the OPC was extended to 20 µm by insertion of a potentiometer on the power supply board. A toggle switch on the back apron of the instrument was wired to the wiper connecting the added potentiometer to the existing one so that the range could be selected from outside of the instrument. The effect of this alteration was to increase the intensity of the light source located at one end of the optics unit which supplies the scattering light to the sample volume.

3. The digital signal to the OPC pixel tubes, which display total counts at a preselected channel, was tapped and connected to an digital to RS232 convertor and from there to a TRS-80 personal computer. The computer controlled data aquisition and storage.

Ragweed pollen, glass beads, and ammonium fluorescein particles were the test aeorosols. The pollen and glass beads were generated in a simple fluidized bed generator. Monodisperse ammonium fluorescein, having an aeorodynamic diameter of 20 µm, was generated using a TSI Model Vibrating Aerosol Generator.

Glass beads with a median aerodynamic diameter of 20 µm were separated from Potter Industries Inc., 5000 Series glass beads using a

water sedimentation technique. The final test aerosol had a geometric standard deviation of 1.3. Figure A-1 shows the effect on the glass bead count distribution of the separation technique.

The rates of penetration of the particles with a greased impaction substrate and with an ungreased stainless steel plate in place were compared to the OPC particle count when no impaction plate was in place. A 28.4-liter sample size was used in the pilot study.

Ammonium fluorescein particles were found to rebound from the ungreased surface in significantly higher numbers than did the ragweed pollen. However, greasing the plate with vaseline reduced the ammonium fluorescein and glass bead penetration by more than 30 percent but only reduced the pollen penetration by 10 percent. Glass beads were far more effectively collected on the greased plate than were the other two materials. Even with a greased impaction plate, the penetration of ammonium fluorescein was greater than 25 percent of challenge concentration. Figure A-2 is a bar graph showing relative bounce of the particle collector combinations, where percent penetration is defined as:

$$\frac{\text{number of particles passing the collector}}{\text{number of particles in challenge air stream}}$$

expressed as a percentage.

A study of the effect of particle loading on a greased impactor plate was conducted using pollen and ammonium fluorescein particles. The greased substrate was left in place over a 20-min period, while 20 consecutive 1-min particle penetration counts were taken. Challenge concentration was measured in the same manner with no collector in place. Samples from challenge and bounce sequences were paired on the basis of their respective positions in the sample time series to determine per cent penetration. Ammonium fluorescein particle penetration increased rapidly and reached the test limit of 50 percent within 8 minutes. The pollen penetration showed no increasing trend over the 20-min period. The results of the loading study are plotted in Figure A-3, where Cimp = the number of particles passing the collector plate, and C_o = the number of particles in the challenge concentration.

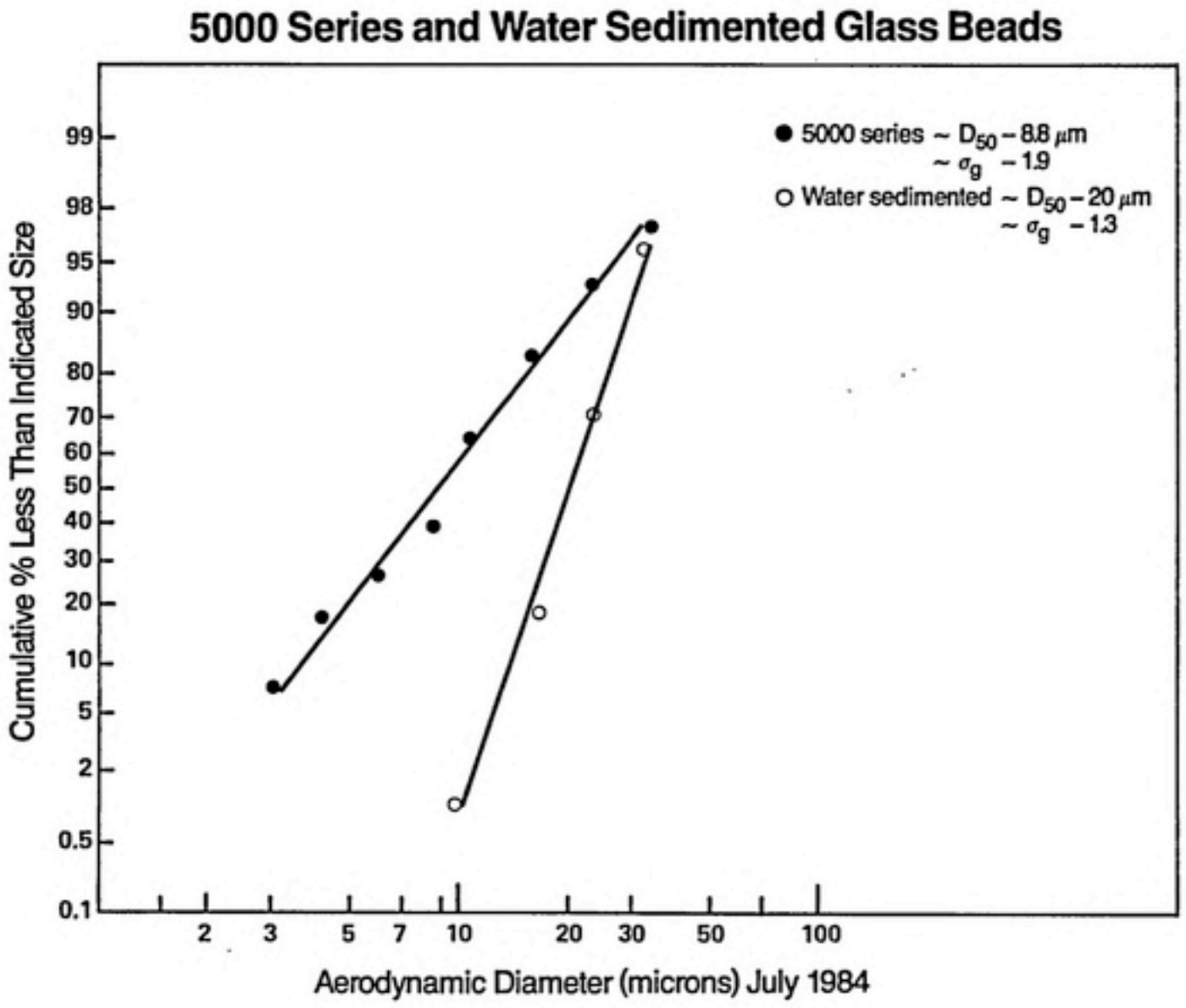
5000 Series and Water Sedimented Glass Beads
● 5000 series ~ D_{50} – 8.8 μm
~ σ_g – 1.9
○ Water sedimented ~ D_{50} – 20 μm
~ σ_g – 1.3
Cumulative % Less Than Indicated Size
99
98
95
90
80
70
60
50
40
30
20
10
5
2
0.5
0.1
2
3
5
7
10
20
30
50
100
Aerodynamic Diameter (microns) July 1984

Figure A-1.

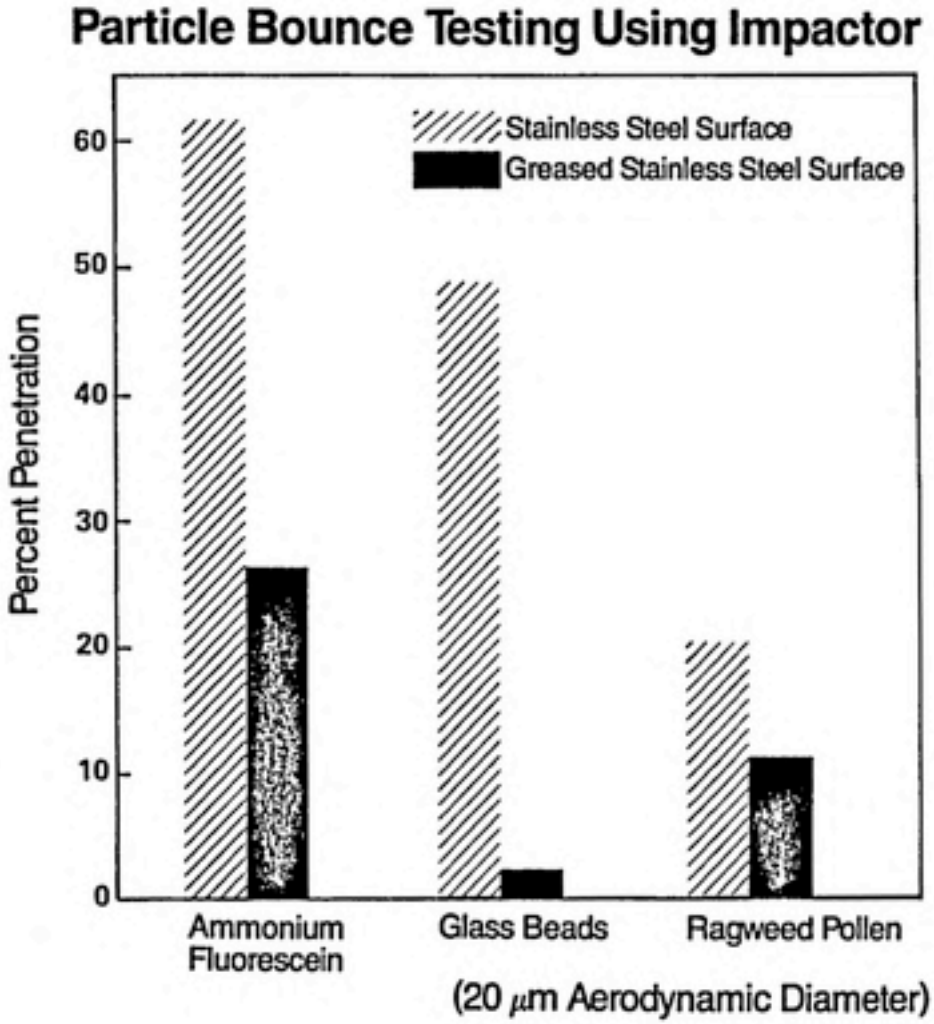
Particle Bounce Testing Using Impactor
Stainless Steel Surface
Greased Stainless Steel Surface
Percent Penetration
60
50
40
30
20
10
0
Ammonium Fluorescein
Glass Beads
Ragweed Pollen
(20 μm Aerodynamic Diameter)

Figure A-2.

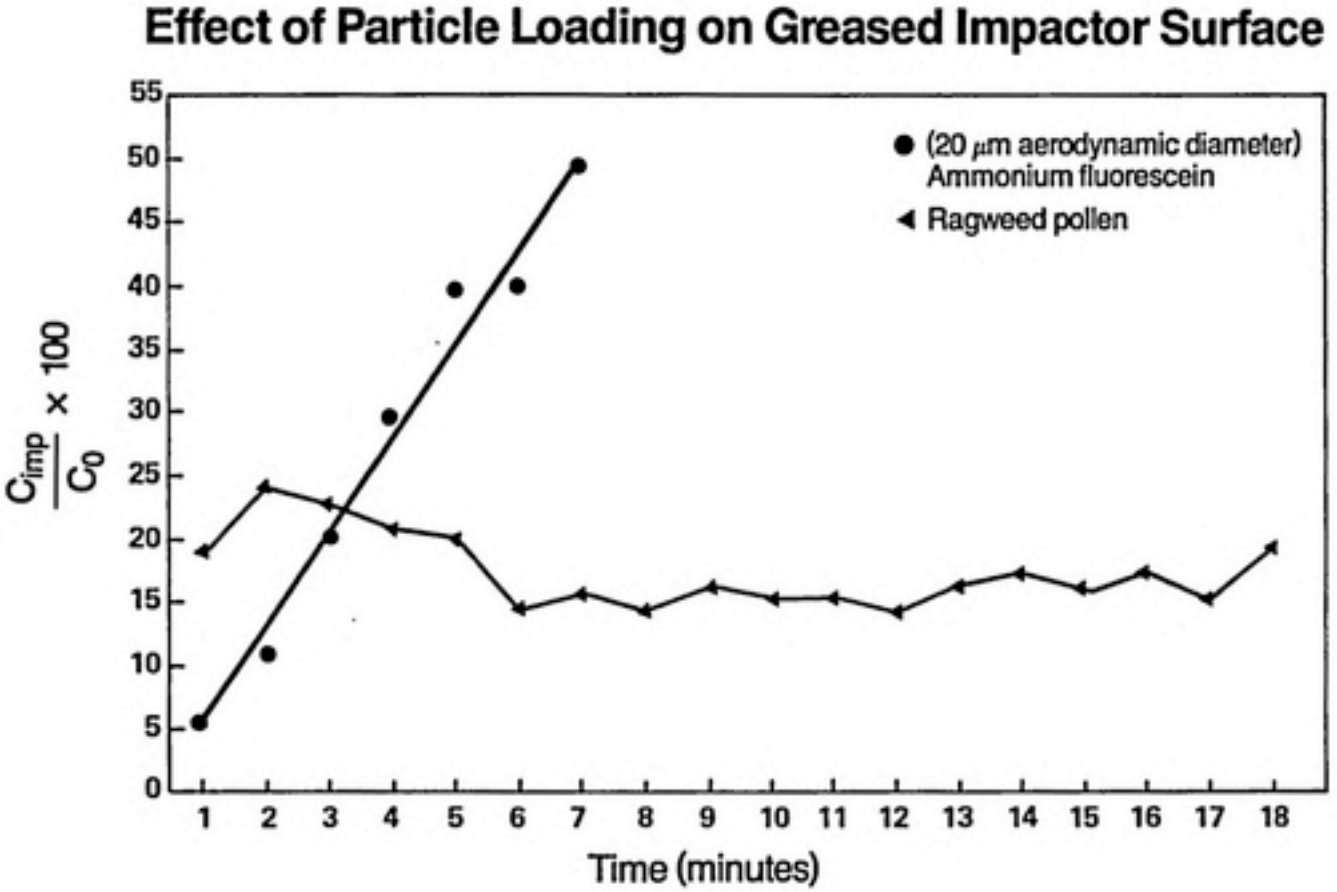
Effect of Particle Loading on Greased Impactor Surface
● (20 μm aerodynamic diameter) Ammonium fluorescein
◀ Ragweed pollen
$\frac{C_{imp}}{C_0} \times 100$
0
5
10
15
20
25
30
35
40
45
50
55
1 2 3 4 5 6 7 8 9 10 11 12 13 14 15 16 17 18
Time (minutes)

Figure A-3.

The following conclusions were drawn from the pilot study test results:

1. Particle bounce can reasonably be studied using an OPC and specially fitted impactor. Relative particle bounce appears to be a function of particle material, and collection surface and difference in materials' penetration is sufficiently large to allow the use of an OPC.

2. Glass beads generated in a fluidized bed showed a decrease in concentration over time as the quantity of beads in the bed was reduced. Consequently, an improved glass bead generation system capable of maintaining concentration constant over a period of several hours was required to adequately study bounce effects.

3. The aerosol concentration should be kept low during particle bounce studies to avoid loading the substrate with the test particles, since particle loading affects particle bounce and masks the bounce induced in a given particle-collector combination.

APPENDIX B

Peformance Testing of the Timbrell Generator

A modified Timbrell asbestos generator (Timbrell, et al., 1968) was tested for the following performance requirements:

1. The generator must deliver a constant concentration of glass beads for a minimum test period of 20 min.
2. The generator must be able to operate continuously for a minimum of two hours.
3. The generator must not alter the size distribution the feed material.
4. It would be advantageous if the concentration delivered by the generator could be altered by changing one or more operating parameters.

The generator was operated with a blade speed of 3450 rpm, a dispersion air flow rate of 40 lpm and a dilution air flow rate of 4 lpm. The air was supplied from a compressor at a pressure of 30 psig and was dried and filtered upstream of the neutralizer.

The glass beads used were water sedimendation separated having a mean aerodynamic diameter of 20 μm and a geometric standard deviation of 1.3 (Figure A-1). The feed material was conditioned by baking it in an oven at 200° C for one hour and then storing it in a dessicator overnight.

The bead stream from the generator was sampled from an open duct with a Climet 208 OPC over a 20-min time period in one-minute intervals. The feed rate of the syringe pump was increased, and the experiment was repeated. Figure B-1 shows a of plot concentration over time for the two experiments with the upper curve representing a higher syringe pump setting.

A sample from the bead stream was collected on glass microscope slides at various times during a two-hour period and beads were sized under an optical microscope using a New Porton Graticule which had been

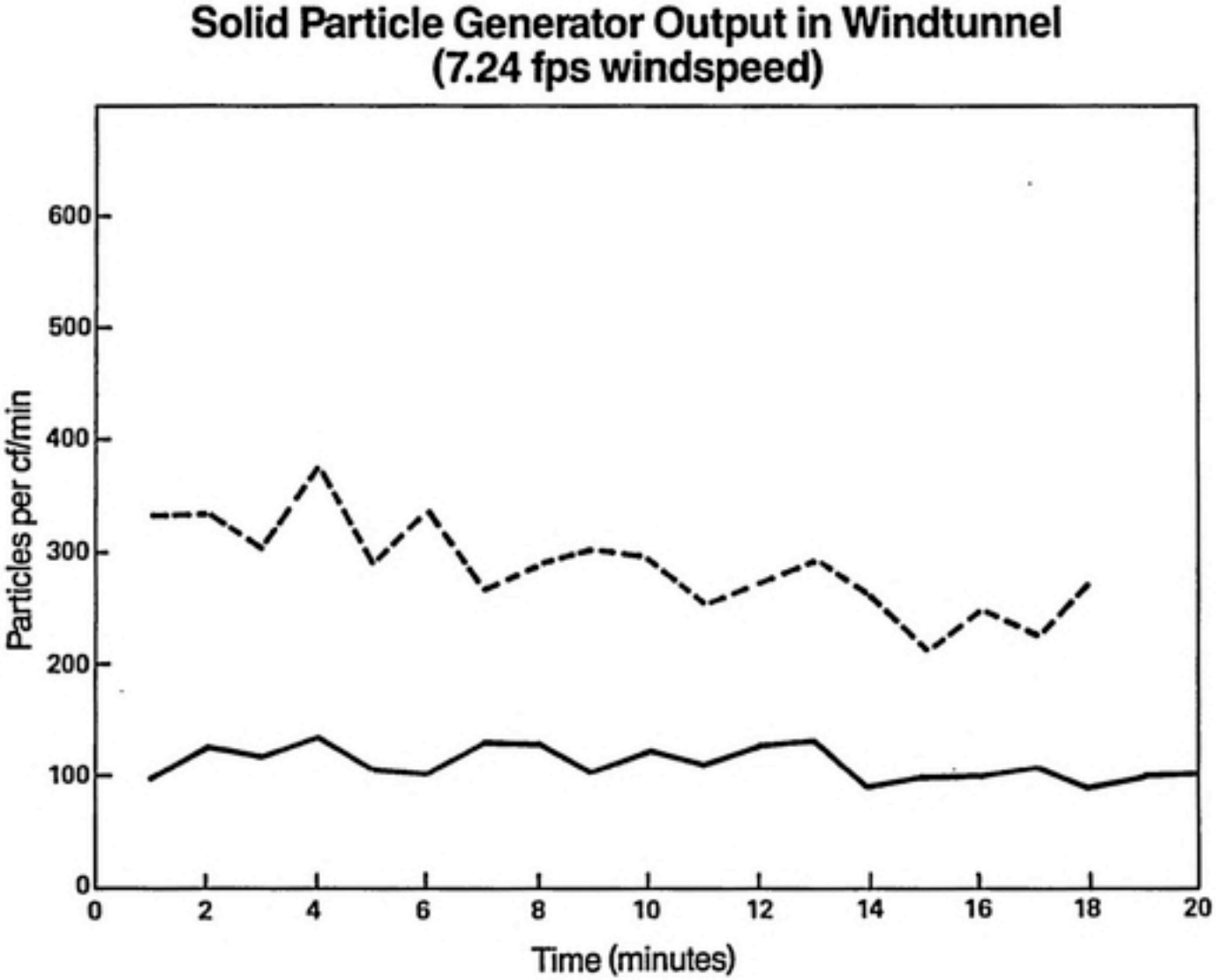
Solid Particle Generator Output in Windtunnel
(7.24 fps windspeed)
Particles per cf/min
600
500
400
300
200
100
0
0
2
4
6
8
10
12
14
16
18
20
Time (minutes)

Figure B-1.

calibrated against a stage micrometer. No significant difference was found between the samples taken of the aerosol and the raw feed material. The generator was found to meet the four stated performance requirements.